



Seismotectonics of Sulawesi, Indonesia

Yopi Serhalawan^{a,b}, Po-Fei Chen^{a,*}

^a Department of Earth Sciences, National Central University, Taoyuan, Taiwan

^b The Indonesian Agency for Meteorological, Climatological and Geophysics, Indonesia

ARTICLE INFO

Keywords:

Seismotectonics of Sulawesi
The latest Miocene collision
Seismicity distributions
Types of focal mechanisms

ABSTRACT

Sulawesi Island, located in eastern Indonesia, lies at the triple junction of the Australian, Sunda, and Philippine Sea plates. It exhibits a distinctive K-shape, with each arm having undergone independent geological evolution. Driven by the latest Miocene collision (~5 Ma) between the Banggai-Sula microcontinent and the East Arm, the deformation is accommodated by the corresponding motion of individual blocks at various locations, resulting in specific patterns of seismic moment release. In this study, we investigate the distributions of shallow earthquakes (< 60 km) based on the ISC-EHB and BMKG catalogs, as well as the focal mechanisms based on the GCMT catalog, to study the seismotectonics of Sulawesi. The results are grouped into five regions with characteristic seismic patterns well corresponding to tectonic signatures and geodetic observations. The main findings can be summarized in two parts. First, thrust earthquakes release seismic energy due to oceanic plate subduction, including, in order of moment release, those along the North Sulawesi Trench to the north, the Makassar Strait Thrust to the west, and the Tolo and Buton Thrust to the southeast. Notably, there is a seismic gap near the center of the North Arm that may indicate potential risk for damaging earthquakes, while those of the Batui Thrust are only minor. The second part involves left-lateral strike-slip motions along the Central Sulawesi Fault System. The occurrence of the 2018 Mw 7.6 Palu earthquake not only filled the gap of seismic deficiency on the Palu-Koro fault but also triggered overall seismic activity in Sulawesi. Additionally, note the low seismicity on the segment offshore northwest Sulawesi, which may be beyond the high relative motion between the Makassar and North Sula Block.

1. Introduction

Sulawesi Island, located in the eastern Indonesian archipelago, is situated at the triple junction of three tectonic plates: the Indian-Australian, Sunda, and Philippine Sea (Fig. 1a). This distinctive “K” shape of the island has resulted in a complex and dynamic geological history (Hall, 2012). The island can be divided into two provinces: Western Sulawesi (North and South Arms) dominated by plutono-volcanic rocks, and Eastern Sulawesi (East and Southeast Arms) characterized by ophiolites and metamorphic belts (Otofujii et al., 1981). The plutono-volcanic rocks of Western Sulawesi were mostly produced by the northwest subduction of the Indian Oceanic Lithosphere during the Paleogene, which ceased in the Early Miocene due to the collision between the northern edge of the Australian continental plate (Sula Spur) and the North Arm of Sulawesi (referred to as the “Early Miocene collision” hereafter) (van Leeuwen and Muhardjo., 2005; Hall and Sevastjanova, 2012). Eastern Sulawesi’s geology developed after this collision (Silver et al., 1983a).

In the Middle Miocene, the Banda slab rollback fragmented the Sula Spur into several microcontinents, leading to the collision of two microcontinents with Eastern Sulawesi: The Buton-Tukang Besi microcontinent with the Southeast Arm (~11 Ma) and the Banggai-Sula microcontinent with the East Arm (~5 Ma) (Fortuin et al., 1990; Hall, 2002). The latter is referred to as the “Latest Miocene collision” hereafter. This collision triggered significant deformations, including the initiation of clockwise rotation of the Northern Blocks (North Sula and Manado) and the counterclockwise rotation of the Southern Blocks (Makassar, East Sula, and Banda Sea) (Fig. 1b) (Socquet et al., 2006). This collision also initiated the Celebes Sea subduction along the North Sulawesi Trench and the formation of the Central Sulawesi Fault System (Palu-Koro and Matano Faults) (Walpersdorf et al., 1998a, 1998b).

Seismic activities in and around Sulawesi are not only vigorous but also versatile, reflecting its complex tectonics (Fig. 1c). In this study, our aim is to understand the tectonic forces driving the occurrences of earthquakes by analyzing earthquake distributions and types of focal mechanisms. Furthermore, we will use the results to better constrain

* Corresponding author.

E-mail address: bob@ncu.edu.tw (P.-F. Chen).

<https://doi.org/10.1016/j.tecto.2024.230366>

Received 30 July 2023; Received in revised form 27 May 2024; Accepted 29 May 2024

Available online 1 June 2024

0040-1951/© 2024 Elsevier B.V. All rights reserved, including those for text and data mining, AI training, and similar technologies.

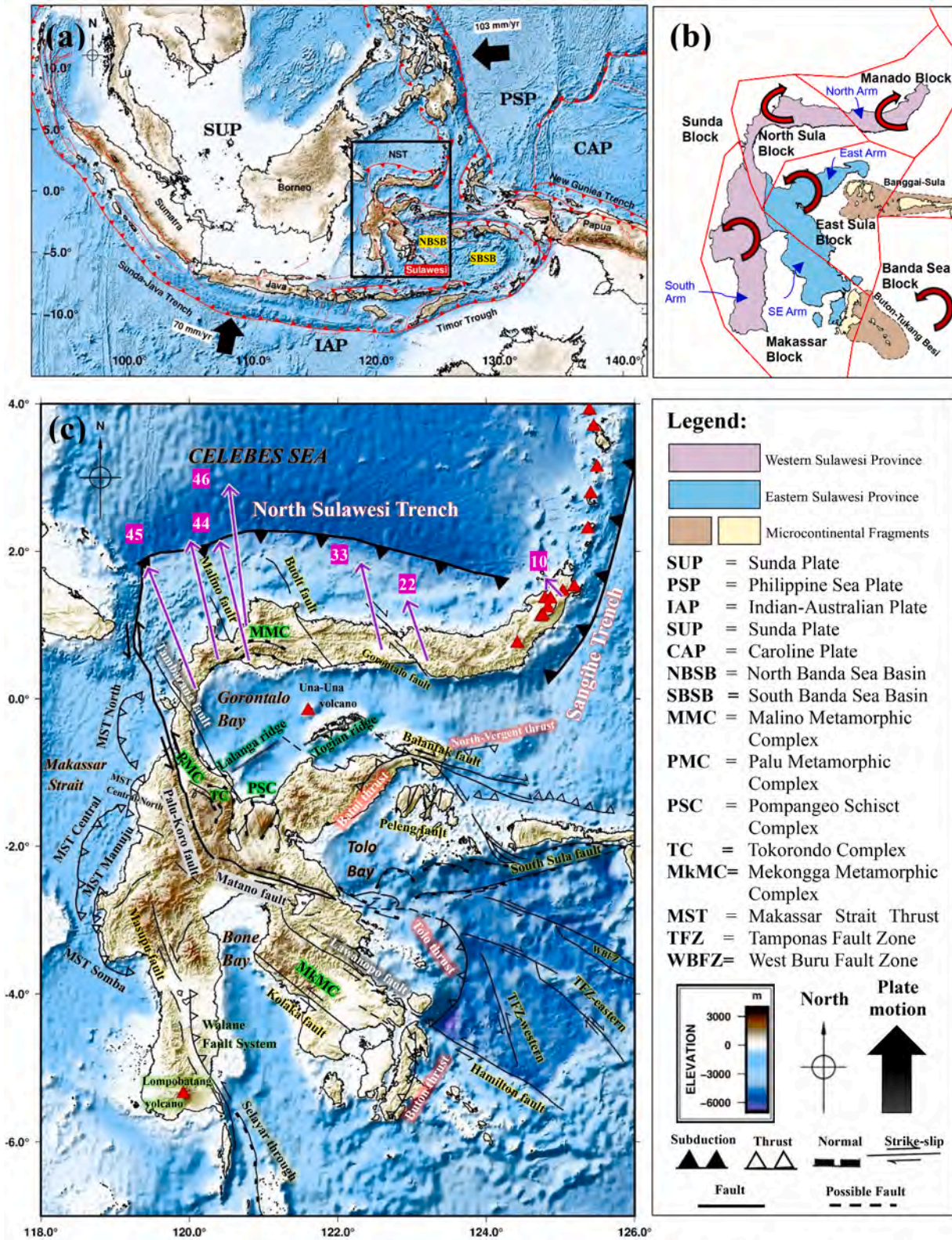


Fig. 1. (a) Principal tectonic map of Indonesia. Black arrows represented the plate motion of three plates (IAP, PSP, CAP) relative to the SUP. The rate of plate motions based on DeMets et al. (2010) and Koulali et al. (2016). (b) Simplified tectonic division of Sulawesi Island, modified after Otofuiji et al. (1981). The red line depicts the tectonic blocks from Socquet et al. (2006). The red curved arrows represent block rotations relative to Sunda Block. (c) The tectonic settings of Sulawesi. The tectonic structures were taken from Hall and Wilson (2000); Watkinson et al. (2011); Pholbud et al. (2012); Jaya (2014); Camplin and Hall (2014); Irsyam et al. (2020); Hall (2018); Titu-Eki and Hall (2020); Hutchings and Mooney (2021). Topography/bathymetry data were obtained from Tozer et al. (2019). The purple arrow with a number near the tips is the GPS velocity (mm/s) of Socquet et al. (2006) relative to Sunda Block. The red triangles represent volcanoes from the Smithsonian Institution Global Volcanism Program (Siebert and Simkin, 2002). (For interpretation of the references to colour in this figure legend, the reader is referred to the web version of this article.)

tectonic scenarios in Sulawesi. The seismotectonic studies here address issues such as (but not limited to): (1) strain accumulation and seismic behavior of the CSFS, particularly focusing on the role of the Mw 7.6 Palu earthquake on September 28th, 2018, (2) the potential for future tsunamigenic earthquakes along the NST, (3) seismic activity associated with the latest Miocene collision. The results derived from these analyses are examined within the framework of (a) tectonic and geological structures, (b) topography and bathymetry information, (c) models of slab subduction, (d) finite fault models of significant earthquakes, (e) seismic tomography results, and (f) distributions of volcanoes, aiming to achieve a comprehensive understanding of Sulawesi seismotectonics.

Results are focused on earthquakes with depths shallower than 60 km depth. We defer those with depths >60 km to another study. The distributions and types of shallow earthquakes (< 60 km) generally agree with the tectonic configurations of Sulawesi, with the left-lateral motions of the PKF (Palu-Koro Fault) and the subduction of the Celebes Sea plate being the most active zones. The northernmost segment of the PKF and the central segment of the NST (121°E - 121.7°E) exhibit

zones of relatively low seismic activity, which can be explained by different mechanisms. We note that overall seismicity in and around Sulawesi increased significantly after the occurrence of the Palu earthquake on 28 September 2018 (Mw 7.6).

2. Tectonics and geological settings of Sulawesi

Sulawesi Island has commonly been subdivided into four main tectonic provinces based on its tectonic and geological structure: the West-Sulawesi Plutono-Volcanic Arc, the Central Sulawesi metamorphic belt, the East Sulawesi ophiolite, and the microcontinental blocks of Banggai-Sula and Buton-Tukang Besi (Hamilton, 1979; Hall and Wilson, 2000) (Fig. 2). The West-Sulawesi Plutono-Volcanic Arc, which is equivalent to the West Sulawesi Province mentioned in the Introduction, consists of the South and North Arms. Both arms are dominated by plutonic and volcanic rocks. However, the characteristics and evolution of the South and North Arms can still be distinguished based on their different basement lithologies, magma types, and sediment provenances.

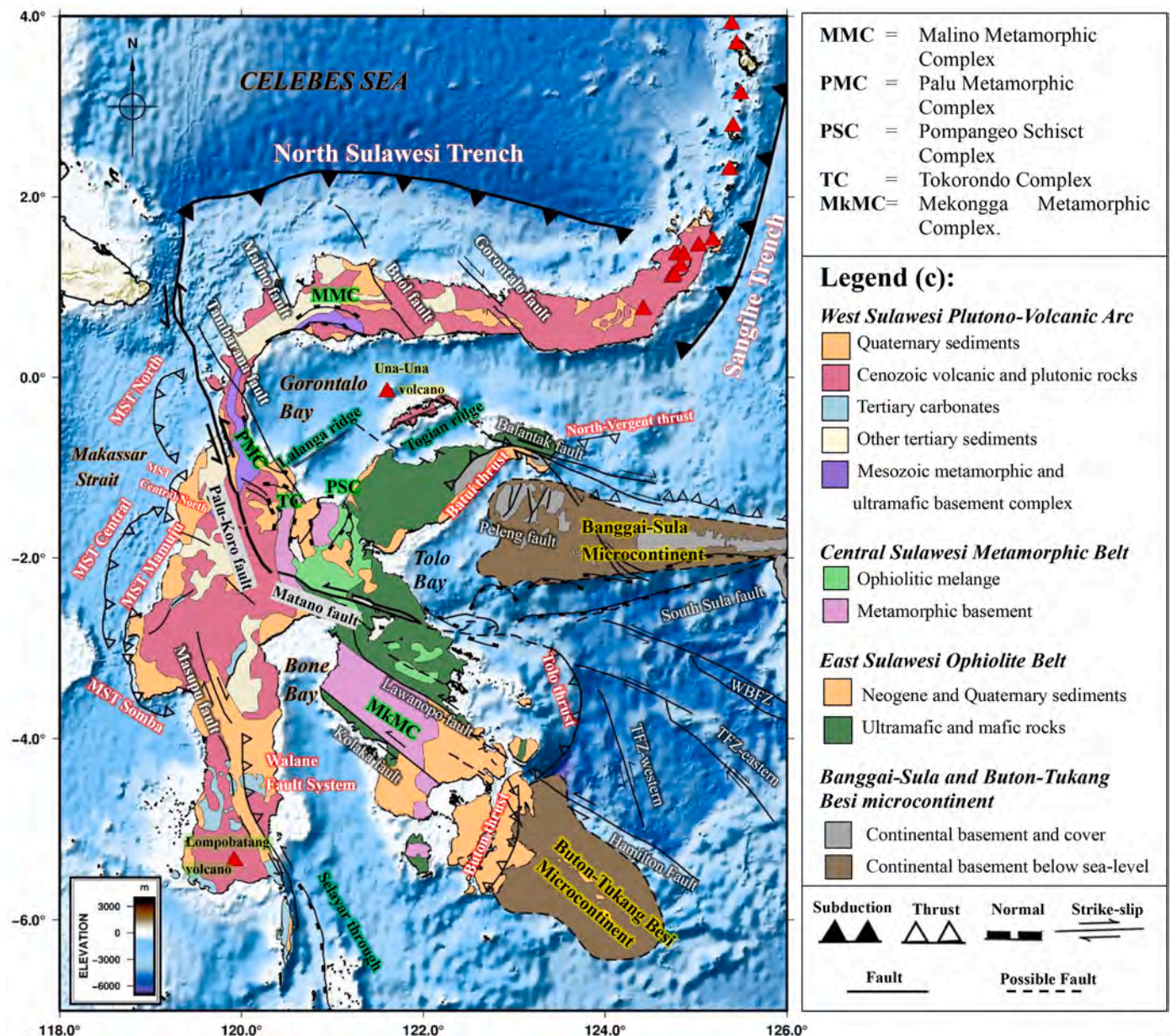


Fig. 2. Summary geology of Sulawesi. The geological structure has been modified after Hall and Wilson (2000); Watkinson et al. (2011). The tectonic structures and volcanoes are identical to Fig. 1c.

The South Arm of Sulawesi originated from the Australian margin of Gondwana, which underwent rifting in the late Jurassic period and subsequently docked to the Sunda plate in the Late Cretaceous. It further developed from the southeastern tip of the Sunda plate, which experienced rifting due to the opening of the Makassar Strait in the Middle Eocene (van Leeuwen et al., 2007, 2016). During the Early Paleocene until the Mid-Oligocene, the South Arm exhibited calc-alkaline magmatism, which is typically associated with subduction behavior. This magmatism is proposed to be related to the northwestward subduction of the Indian oceanic lithosphere beneath the South Arm of Sulawesi (Polvé et al., 1997). However, during the Oligocene, there was a counterclockwise rotation of the South Arm, which transformed the active continental margin into a predominantly strike-slip margin. As a result, the subduction ceased, and no late Oligocene calc-alkaline magmatism is recorded in this area (van Leeuwen and Muhardjo., 2005).

On the other hand, in the North Arm of Sulawesi, the northward subduction of the Indian oceanic lithosphere beneath it commenced in the Early Oligocene. As the oceanic lithosphere was consumed by subduction, a collision between the Australian continent (Sula Spur) and the North Arm of Sulawesi occurred, resulting in the formation of the Early Miocene collision (Nugraha et al., 2022). The basements of the North Arm of Sulawesi are predominantly underlain by an oceanic crust associated with the back-arc spreading of the Celebes Sea in the Middle Miocene, as indicated by geochronological and geochemical data (Zhang et al., 2022).

What developed ensuing the Early Miocene collision are the Central Sulawesi Metamorphic Belt and the East Sulawesi Ophiolite. The former consists of the Pompango Schist Complex (PSC), the Mekongga Metamorphic Complex (MkMC), and an ophiolitic mélange mainly located at the junction of the East and Southeast Arms (Fig. 2). PSC and MkMC to the west are predominantly metamorphic rocks underlain by the crust of the Australian continents, while the ophiolitic mélange to the east, overlying the metamorphic sole represents the initial stages of oceanic subduction (Parkinson, 1996; Parkinson, 1998). The latter constitutes a dominating sequence of the East and Southeast Arms, resulting from obduction onto the Sula Spur continent by the ocean north of it (Silver et al., 1983a).

Likewise, the north-dipping Indian Oceanic slab detached at ~200 km due to the Early Miocene collision. While the lower slab sank into the lower mantle, remnants of the upper slab have persisted until now, specifically the Sula slab. This is evidenced by combined observations of seismicity, tomography, and geology (Hall and Spakman, 2015). On the other hand, the rollback of the Banda slab, which occurred further westward, initiated around 15–12 Ma (Hall and Sevastjanova, 2012) and played a significant role in shaping the tectonics of modern Sulawesi. The rollback not only initiates the opening of the North and South Banda Seas, which formed around 12.5–7 Ma and 6.5–3.5 Ma, respectively (Hinschberger et al., 2000, 2001), but also induces stretching and fragmentation of the Sula Spur. As mentioned in the Introduction, the present block rotation in Sulawesi, subduction of the Celebes Sea plate along NST, and development of CSFS are all have been initiated by the latest Miocene collision (~5 Ma) between the Banggai-Sula micro-continent and the East Arm.

Current fault systems in and around Sulawesi are a result of the latest Miocene collision, which has been monitored through geodetic studies (Walpersdorf et al., 1998a, 1998b; Socquet et al., 2006). The most prominent fault system is the Central Sulawesi Fault System (CSFS), extending southeasterly and encompassing the Palu-Koro, Matano, and Tolo thrust. The Palu-Koro and Matano faults, classified as left-lateral faults, accommodate the relative motions of MKB-NSB and MKB-ESB, respectively. Additionally, the Tolo thrust, which dips to the west, results from the convergence between the North Banda Sea and the Southeast Arm.

In the North Banda Sea, several faults have been identified based on remote sensing observations (Titu-Eki and Hall, 2020). These faults include the West Buru Fault Zone (WBFZ), the Tamponas Fault Zone

(TFZ), and the Hamilton Fault Zone (HFZ) (Fig. 2, in southerly order). To the south of the Matano fault, the Lawanopo and Kolaka faults trend northwest to southeast and are separated by the MkMC. While Socquet et al. (2006) interpret the Lawanopo fault as the boundary between MKB-ESB, recent geodetic studies (Rahmadani et al., 2022) have only observed a slip rate of approximately 0.1 mm/yr, categorizing it as non-active (Bellier et al., 2006; Natawidjaja and Daryono, 2015). On the other hand, the Kolaka fault consists of several segments dominated by strike-slip behavior with slightly normal components in the center and the southeastern end of the fault (Watkinson and Hall, 2017).

Faults in the South Arm of Sulawesi distribute into two groups – the Makassar Strait Thrust (MST) to the west and the Walane Fault System (WFS) to the south (Fig. 2). The MST, including North, Central, Mamuju, and Somba segments, is an east-dipping thrust fault bordered the Makassar Strait (Irsyam et al., 2020), with a newly identified segment between the North and Central (MST Central-North) by Hutchings and Mooney (2021). The NNW-SSE trending WFS consists of the Masupu fault to the north (right-lateral strike slip), and the East Walane Fault (EWF, east-dipping thrust segment to the north and left-lateral strike slip to the south) and the West Walane Fault (WWF, generally strike slip) to the south (Jaya, 2014).

The clockwise rotation of NSB and MB induced by the latest Miocene collision also triggered the subduction of the Celebes Sea, which is part of the Sunda Block, along the NST (Socquet et al., 2006; Hall and Spakman, 2015). The pole of the Sunda Block – NSB/MB relative motion was placed towards the eastern end of the North Arm (Socquet et al., 2006), resulting in westerly increasing convergence rates, evidenced by the right-lateral strike-slip motion of the Gorontalo Fault and the growing thickness of the accretionary wedge to the west (Silver et al., 1983b; Kopp et al., 1999). However, the maximum depth of the Celebes slab is not at the western end but near the center of the NST. Song et al. (2022) proposed that the discrepancy could be due to being out of the North Arm range for the western end and growth space limited by the preexisting Sangihe slab for the eastern end. On the other hand, Greenfield et al. (2021) suggest that variations in gravitational potential energy may also play a key role in influencing the deformation in the northern arm of Sulawesi.

There is no present-day subduction volcanism associated with Celebes Sea subduction. The volcanic chain to the east of the North Arm is due to the subduction of the west-dipping Sangihe slab (Hall, 1996). The active Una-Una Volcano, situated 250 km south of the NST, together with offshore extension and subsidence south of the NST, rapid subsidence offshore in Gorontalo Bay, and exhumation of the PMC, MMC, TC, and PSC, all are results of the Celebes Sea slab rollback since the Pliocene (Cottam et al., 2011; Advokaat et al., 2017; Fig. 2).

3. Dataset and methods

Focusing on the region within 118°–126°E and 7°S–40°N, earthquake data from the ISC-EHB, the BMKG, and the GCMT catalog were sorted out for seismotectonic studies. Additional constraint data related to tectonic structures (Irsyam et al., 2020; Titu-Eki and Hall, 2020; Hutchings and Mooney, 2021), geological features (Hall and Wilson, 2000; Watkinson et al., 2011), topography and bathymetry information (SRTM15+ data; Tozer et al., 2019), slab subduction models (Slab 2.0; Hayes et al., 2018), finite fault models (United States Geological Survey; Hayes, 2017), seismic tomography model (UU-P07 model; Amaru, 2007; Hall and Spakman, 2015), and volcanoes (Siebert and Simkin, 2002) were also included.

We employ the ISC-EHB catalog (Engdahl et al., 2020) to analyze overall seismic distributions between 1964 and 2019, while the period between 2020 and July 2022 is supplemented by the BMKG (Badan Meteorologi, Klimatologi, dan Geofisika) catalog. The ISC-EHB catalog was used because of its incorporation of depth phases (pP, sP, pwP) at each iteration of hypocenter determination, avoiding trade-offs between depth and origin time (Engdahl et al., 1998). The BMKG catalog is

primarily determined through the Locsat method (Bratt and Bache, 1988) implemented in the SeisComP 5 program (Potsdam, 2008) using local-regional stations. For earthquake focal mechanisms and scalar seismic moment between 1976 and August 2022, we obtain data from the GCMT catalog (Dziewonski et al., 1981; Ekström et al., 2012). We homogenized the magnitude of different catalogs into Mw of the GCMT (Mw-GCMT) using established global relations (Scordilis, 2006) for the ISC-EHB and linear regression (Fig. S1a) for the BMKG. As a result, the magnitude of completeness (M_c) of the BMKG events is Mw 3.8 (Fig. S1b), while the minimum magnitude for ISC-EHB catalog is Mw 4.3. Earthquake data were exclusively utilized for the shallow part, limited to depths shallower than 60 km. The focal mechanisms of earthquakes were classified into strike-slip, thrust, and normal types (Frohlich and Apperson, 1992; Chen et al., 2015) (Fig. S2). The shallow part of Sulawesi was further divided into five coherent regions for an analysis of patterns of seismicity and focal mechanisms (Fig. 3).

4. Results

We categorize the shallow part (<60 km) of Sulawesi into five regions and present the results in order.

4.1. Region I (Fig. 4)

The majority of earthquakes here are inter-plate type, associated with the subduction of the Celebes Sea slab, based on two observations: (1) they are located offshore north of the North Arm and distributed parallel to the NST at depths of around 20–60 km (Hayes et al., 2018), and (2) almost all significant earthquakes exhibit a focal mechanism of a shallowly south-dipping plane with a trench-parallel strike. Among them, the largest event is the 1996 Mw 7.9 earthquake near the western end of the subduction zone, where the convergence rate reaches its maximum value with the direction to the north relative to the Sunda block (Socquet et al., 2006). The strike-slip events in this region, although their distribution is not entirely clear, suggest a variation in the convergence rate along the trench of the Celebes Sea subduction. Some of them might be related to the crustal earthquake.

On the other hand, seismic activity in the crust of the overriding plate is low, despite the estimated ~11 mm/yr rate of right-lateral motion around the Gorontalo Fault (Socquet et al., 2006). It is noted that a historical earthquake with a magnitude of 7.2 in 1941 occurred at the Gorontalo fault at a depth of 35–50 km (ISC On-Line Bulletin). The uncertainty and insufficiency of earthquake data from back then make the origin of the event undetermined. In any case, the potential of a future large earthquake on the Gorontalo Fault cannot be ruled out.

4.2. Region II (Fig. 5)

The main driving mechanism of earthquakes here is the left-lateral strike-slip Palu-Koro Fault, which is the main active structure in Sulawesi accommodating approximately 42 mm/yr of MKB-NSB relative motion (Socquet et al., 2006). If the motion is solely locked on a single fault, the frequency of earthquakes is predicted to be one magnitude 7 event every 100 years (Socquet et al., 2006), which is not seen in the trenching study of the Palu area (Bellier et al., 2001). Furthermore, the seismic moment release since 1964 was apparently low before the occurrence of the 2018 Mw 7.6 Palu earthquake, with only ~5 earthquakes with Mw > 6 from the GCMT catalog. Such seismic deficiency is even worse when considering that some of the Mw > 6 events are associated with the Tambarana fault, the Sapu Valley fault, the northern segment of the Palu-Koro fault, or the normal faulting type of the pull-apart basin.

However, the 2018 Mw 7.6 Palu earthquake fills the gap of seismic deficiency to some extent and demonstrates the importance of catalog completeness in seismotectonic studies. The Palu event, predominantly characterized by a southerly propagating rupture, featured a primary

asperity located inland south of Palu Beach, evidenced by identifiable surface rupture extending southward (Natawidjaja et al., 2020). The exact location and initiation mechanism of the preceding rupture remain unresolved. While remote-sensing data favor the presence of an unknown, concealed fault (NS-PF in Fig. 5; He et al., 2019), a study integrating field measurements, LiDAR, swath bathymetry, and seismic-reflection suggests that the earthquake originated at the center of the Donggala segment (the yellow line in Fig. 5; Natawidjaja et al., 2020). Irrespective of the exact origin, a substantial amount of the MKB-NSB motion was released during the Palu earthquake. Additionally, recent Coulomb stress studies have revealed that the 1996 Mw 7.9 Minahassa thrust earthquake (northeast of the Palu-Koro Fault) significantly increased the Coulomb stress change at the hypocenter of the 2018 Palu earthquake, making it more susceptible to rupture (Liu and Shi, 2021, 2022).

Lastly, some clusters of normal-type earthquakes existed beneath the Tokorondo complex to the east of the southern Palu-Koro fault, reflecting extensional settings. The largest earthquake (Mw 6.6) in this zone occurred on 29 May 2017, with a southwest-dipping normal mechanism (Wang et al., 2018; Daniarsyad et al., 2021). This earthquake exhibited extensional behavior due to gravitational collapse, which correlated with lateral mass extrusion facilitated by the Palu-Koro fault during the Quaternary (Wang et al., 2018).

4.3. Region III (Fig. 6)

The seismotectonic sources here mainly include the east-dipping Makassar Strait Thrust (MST) offshore west of the South Arm, the Mamasa zone in central, and the Walane Fault System (WFS) in southern South Arm.

The MST accommodates the convergent motion between the Sulawesi and Sunda blocks at rates of 5 to 11 mm/year (Socquet et al., 2006). It is composed of five segments: MST North, MST Central, MST Central-North, MST Mamuju, and MST Somba (Irsyam et al., 2020; Hutchings and Mooney, 2021). Among these segments, MST North experiences the least seismic activity, while MST Central-North exhibits moderate earthquakes predominantly of thrust type. MST Central has shown an increasing seismic activity since September 2020, starting with a magnitude 5 event and culminating in a magnitude 5.5 event. The other two segments, MST Mamuju and MST Somba, experienced the highest magnitudes of 6.7 and 7.1, respectively, with the events occurring in 1984 and 1969. Following 1984, seismicity in MST Mamuju remained inactive until the Mamuju-Majene earthquake on 14 January 2021, with magnitudes of Mw 5.7 and 6.3. In contrast, the last earthquake with a magnitude equal to or >5.0 in MST Somba occurred in 1970, exhibiting a characteristic of seismic silence.

The seismicity in the Mamasa zone exhibited swarm characteristics and was dominated by normal and strike-slip mechanisms simultaneously (Supendi et al., 2019). Due to the Banda slab rollback, this zone experienced a Late Miocene intermediate-felsic magmatic explosion of approximately 7–6 Ma, related to the extension behavior (Zhang et al., 2020). Additionally, the tomography model showed that low-velocity layers densely covered this zone (A-A' profile in Fig. 9). Both are justified by the normal-type mechanism of the Mamasa swarm. The remaining earthquakes of the predominantly right-lateral strike-slip mechanism may be controlled by the north-south trending Masupu fault. Considering the Mamasa swarm, which occurred in November 2018, about one month after the 28 September 2018 Palu earthquake, we suggest that the swarm activity in the Mamasa zone might be correlated with the Palu earthquake. This is also consistent with the positive Coulomb stress change in the Mamasa region transferred by the 2018 Palu earthquake (Wibowo et al., 2020) and the increasing seismicity and seismic moment after the 2018 Palu earthquake (Fig. 10).

To the south, the Walane Fault System (WFS) is expressed by two segments: the East Walane Fault (EWF) and the West Walane Fault (WWF). The EWF segment is more seismically active than the WWF

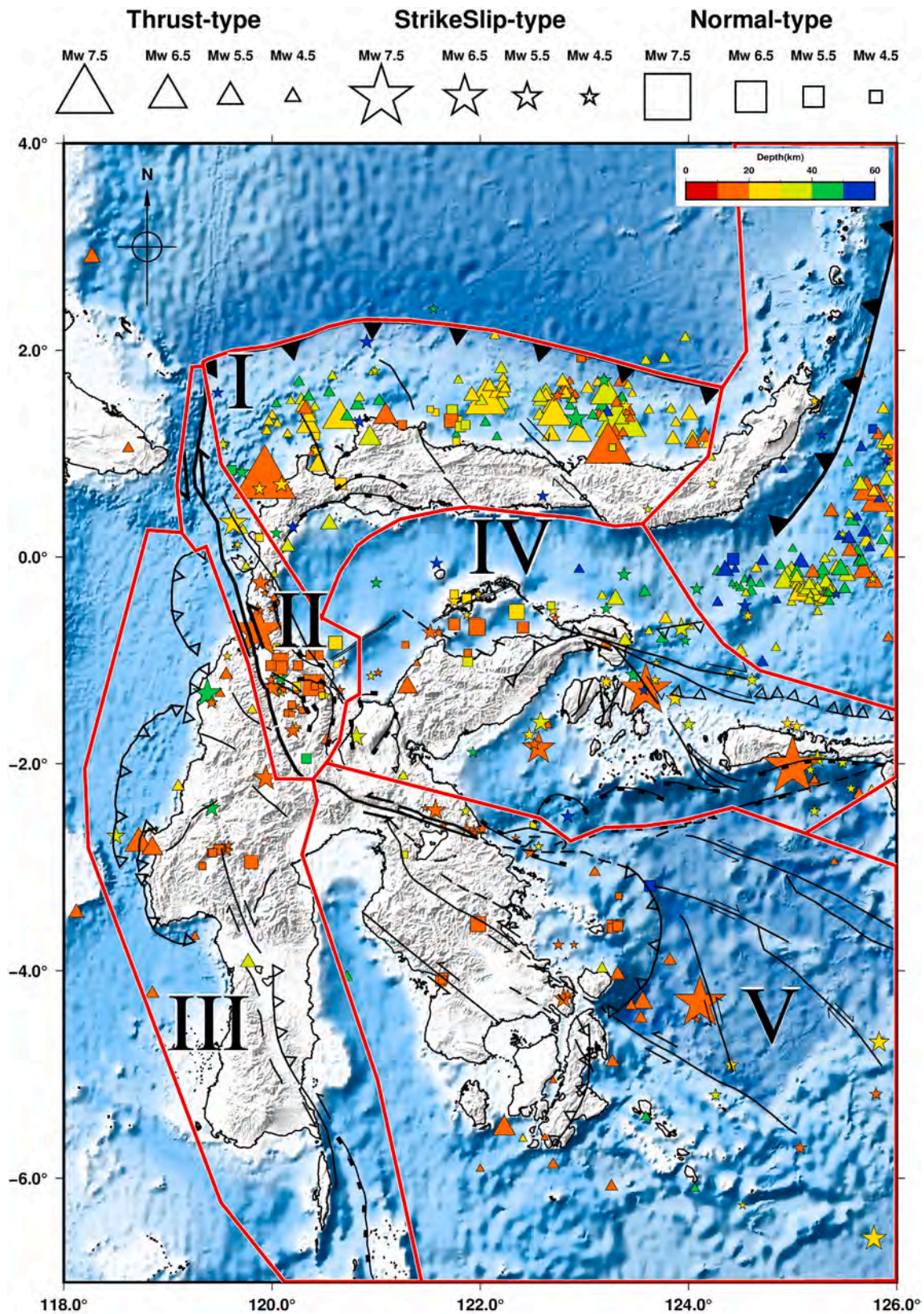


Fig. 3. Distributions of earthquakes from the GCMT catalog (1976–08/2022). The earthquakes are represented by different symbols, scaled to moment magnitude, indicating various types of mechanism (triangle = thrust-type, star = strike slip-type, square = normal-type), with the depth colour-keyed (Classification of mechanisms refer to Fig. S2). The red lines represent the region division of study area (I–V). The tectonic structures are identical to Fig. 1c. (For interpretation of the references to colour in this figure legend, the reader is referred to the web version of this article.)

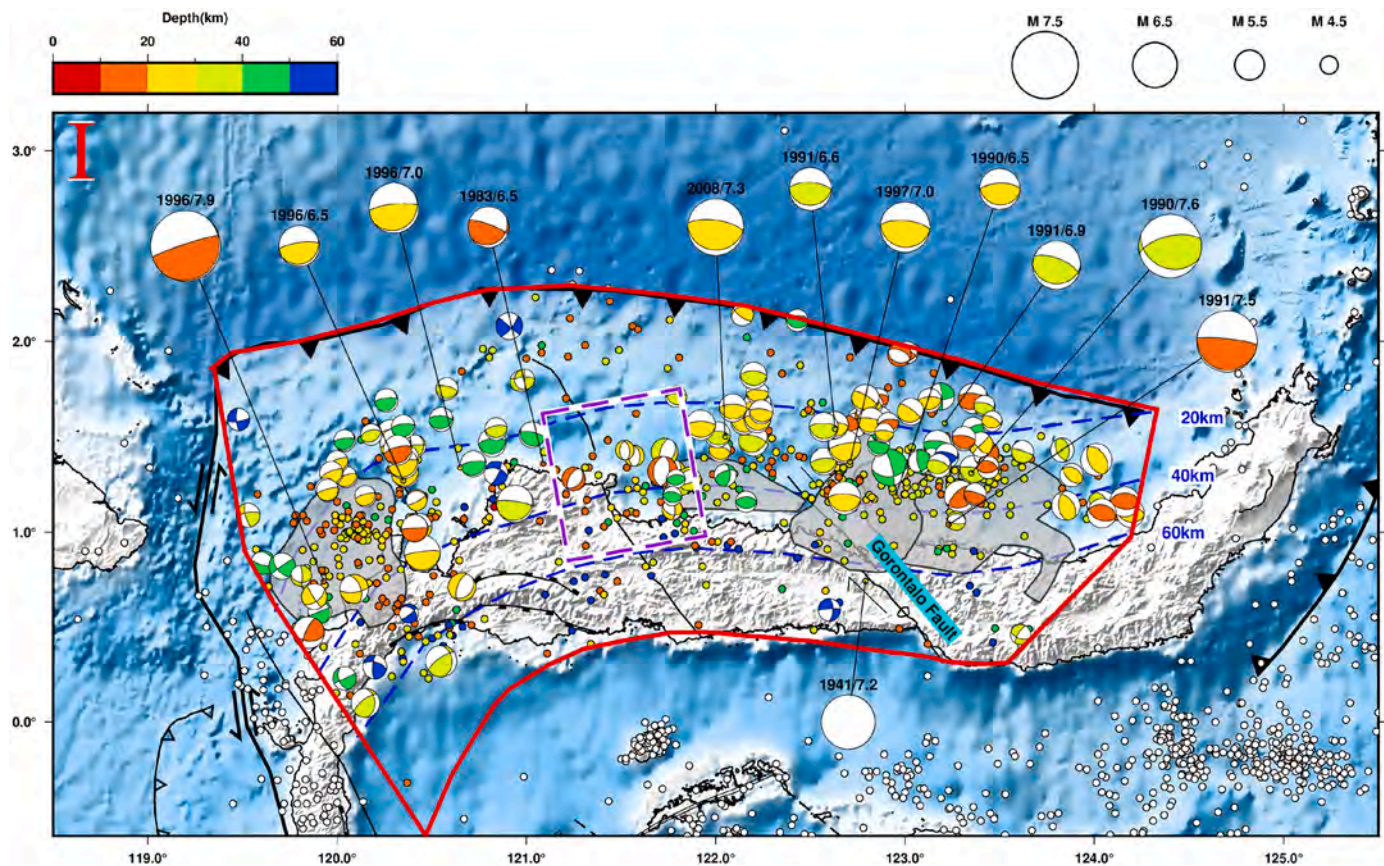


Fig. 4. Earthquake (1964–07/2022) and focal mechanism (1976–08/2022) distributions for the shallow part (<60 km) in Region I (red-line shape). The colour-keyed marks the centroid depth and is scaled by magnitude. The dots represent the seismicity with the depth colour-keyed. The white dots are the seismicity beyond the highlighted region. Earthquakes with $M_w \geq 6.5$ are highlighted with corresponding events labelled (shown as [year/mw]). The highlighted earthquake without focal mechanism (white circle) is the event that occurred before the start time of GCMT catalog. The tectonic structures are identical to Fig. 1c. Blue dashed lines represent slab Benioff zone contours of Celebes sea subduction zone from Hayes et al. (2018). The purple dashed square indicates the area lacking interplate earthquakes. Gray-colored area indicating the ruptured area of these four major events (ordered from the left to the right): 1996/7.9, 2008/7.3, 1991/7.5, 1990/7.6 (USGS; Hayes, 2017; Zheng et al., 2023). (For interpretation of the references to colour in this figure legend, the reader is referred to the web version of this article.)

segment. Overall seismicity of WFS was low, attributed to a slip rate of only 0.5 mm/yr (Rahmadani et al., 2022). Lastly, a few events offshore south of the South Arm are associated with the activity of the Selayar Fault Zone.

4.4. Region IV (Fig. 7)

This region is the site of the latest Miocene collision, where the Banggai-Sula microcontinent collided with the East Arm, and exhibits the most complex seismicity patterns among our study area. The westward translation of the Banggai-Sula microcontinent via the South Sula fault (Hinschberger et al., 2003; Titu-Eki and Hall, 2020) might have triggered the largest earthquake since 1964 (the 29 November 1998 M_w 7.7 earthquake) and could be responsible for the occurrence of other left-lateral strike-slip earthquakes in this zone. On the other hand, the collision was marked by the surface expression of the Batui thrust, Balantak right-lateral strike-slip fault, and Peleng left-lateral strike-slip fault (Simandjuntak, 1986). The 4 May 2000 (M_w 7.5) strike-slip earthquake can be attributed to either the Balantak or Peleng fault due to point source equivalence of two nodal planes. Based on the NE-SW distributions of aftershocks (Fig. S3) and the consistent left-lateral type with that of the Peleng fault, we propose that left-lateral slip on the NE-SW nodal plane is most likely the true fault plane. It is consistent with the finite fault model analysis, which identified NE-SW striking as a true fault plane (Hayes, 2017; <https://earthquake.usgs.gov/earthquakes/eventpage/usp0009sbh/finite-fault>).

To the southwest of the Peleng fault, the Tolo Bay zone was occupied by a cluster of seismicity that became active in April 2019, preceded by the 12 April 2019 M_w 6.8 with a strike-slip mechanism. The last significant seismic activity prior to April 2019 occurred in August 1999, with magnitudes of 6.1 and 5.5. By observing the seismicity patterns and the type of focal mechanisms, we concluded that the off-coast southwestern continuation of the Peleng fault might extend to Tolo Bay, producing the strike-slip mechanism and clustered seismicity with NE-SW trending.

The seismicity near the northern edge of the East Arm was mostly dominated by normal-type earthquakes, possibly related to the Lalanga ridge, the Togian ridge, or several possible faults with extension behavior. Some strike-slip earthquakes in this zone could represent the transform boundary between the Lalanga and Togian ridges. Additionally, other strike-slip earthquakes were likely generated by an unidentified fault. Interestingly, the Batui thrust exhibited a low level of seismicity, and no available solutions are found in the GCMT catalog. In this zone, the last earthquakes with a magnitude greater than five occurred in 1964, 1966, and 1981 with magnitudes 6.7, 6.5, and 5.5, respectively. These are most likely originated from the Batui thrust.

The thrust and strike-slip earthquakes on the northeast side of the Batui thrust might be related to the North-Vergent thrust, the Balantak fault, or other unidentified faults offshore. Conversely, the clustered seismicity on Una-Una Island is associated with the active Una-Una volcano. Rather than being generated by the Celebes subduction, the Una-Una volcano was formed due to crustal thinning related to the

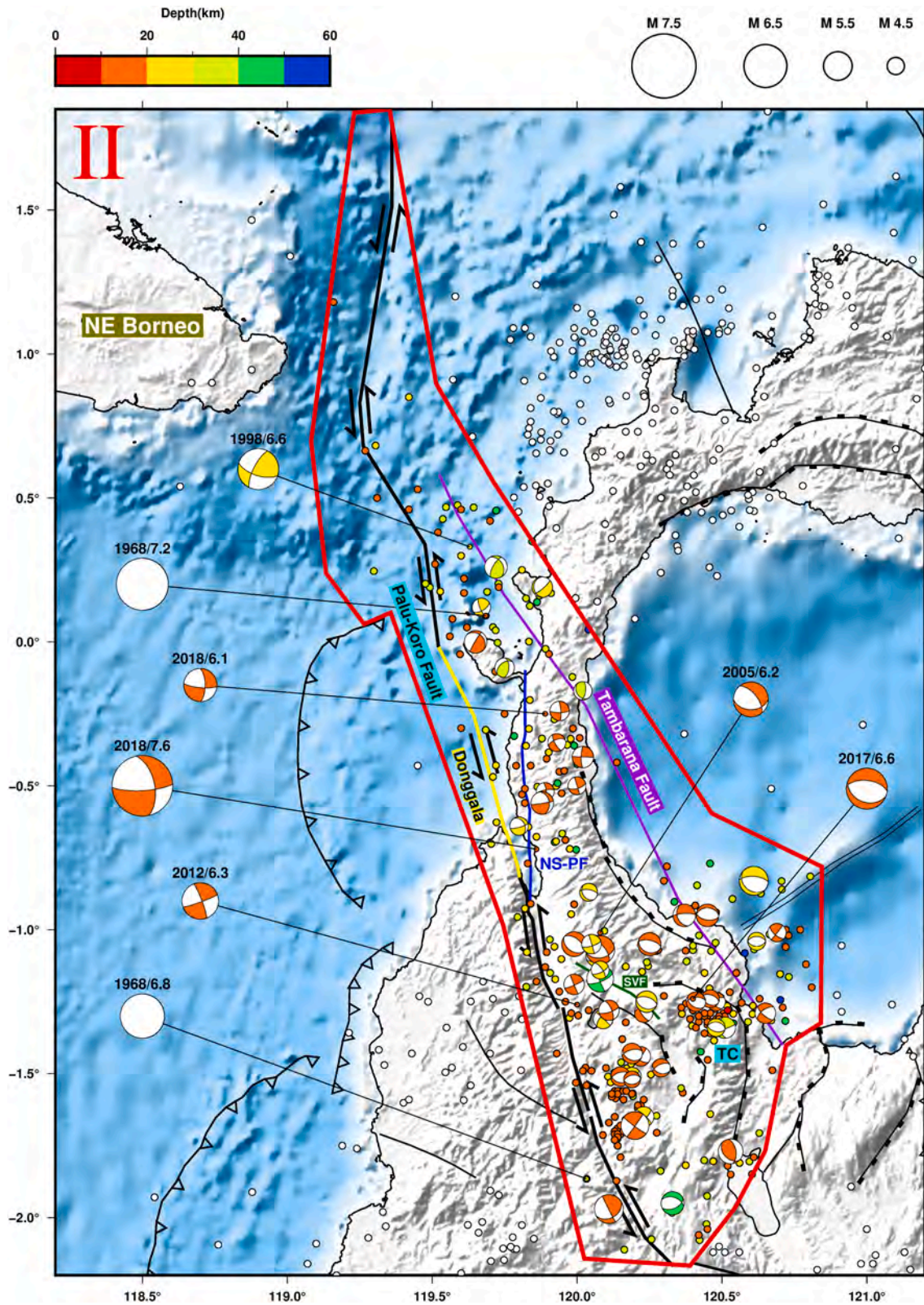


Fig. 5. Similar to Fig. 4 but for region II. Earthquakes with $M_w \geq 6.0$ are highlighted. The blue line denotes the northern segment of Palu-koro fault (NS-PF). The yellow line is the Donggala segment (Part of the major Palu-Koro fault). The purple and green lines are the Tambarana Fault and Sapu Valley fault (SVF), respectively. TC = Tokorondo complex. (For interpretation of the references to colour in this figure legend, the reader is referred to the web version of this article.)

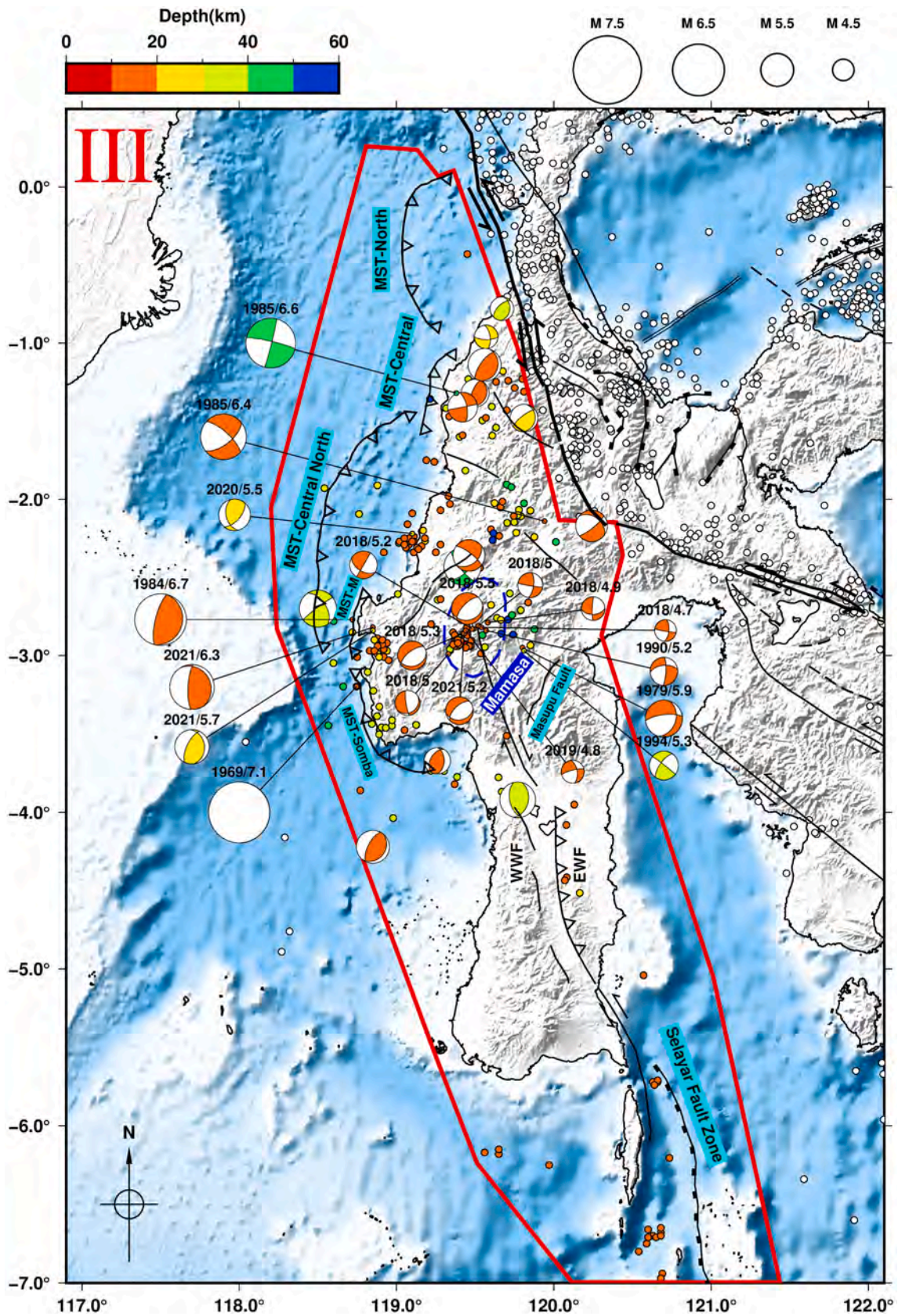


Fig. 6. Similar to Fig. 4 but for region III. Earthquakes with $M_w \geq 6.0$, related to Mamasa swarm, and mentioned in the result are highlighted. The blue dashed line corresponds to swarm activity in the Mamasa zone. MST = Makassar Strait Thrust. MST-M = MST-Mamuju. WWF=West Walane Fault. EWF = East Walane Fault. (For interpretation of the references to colour in this figure legend, the reader is referred to the web version of this article.)

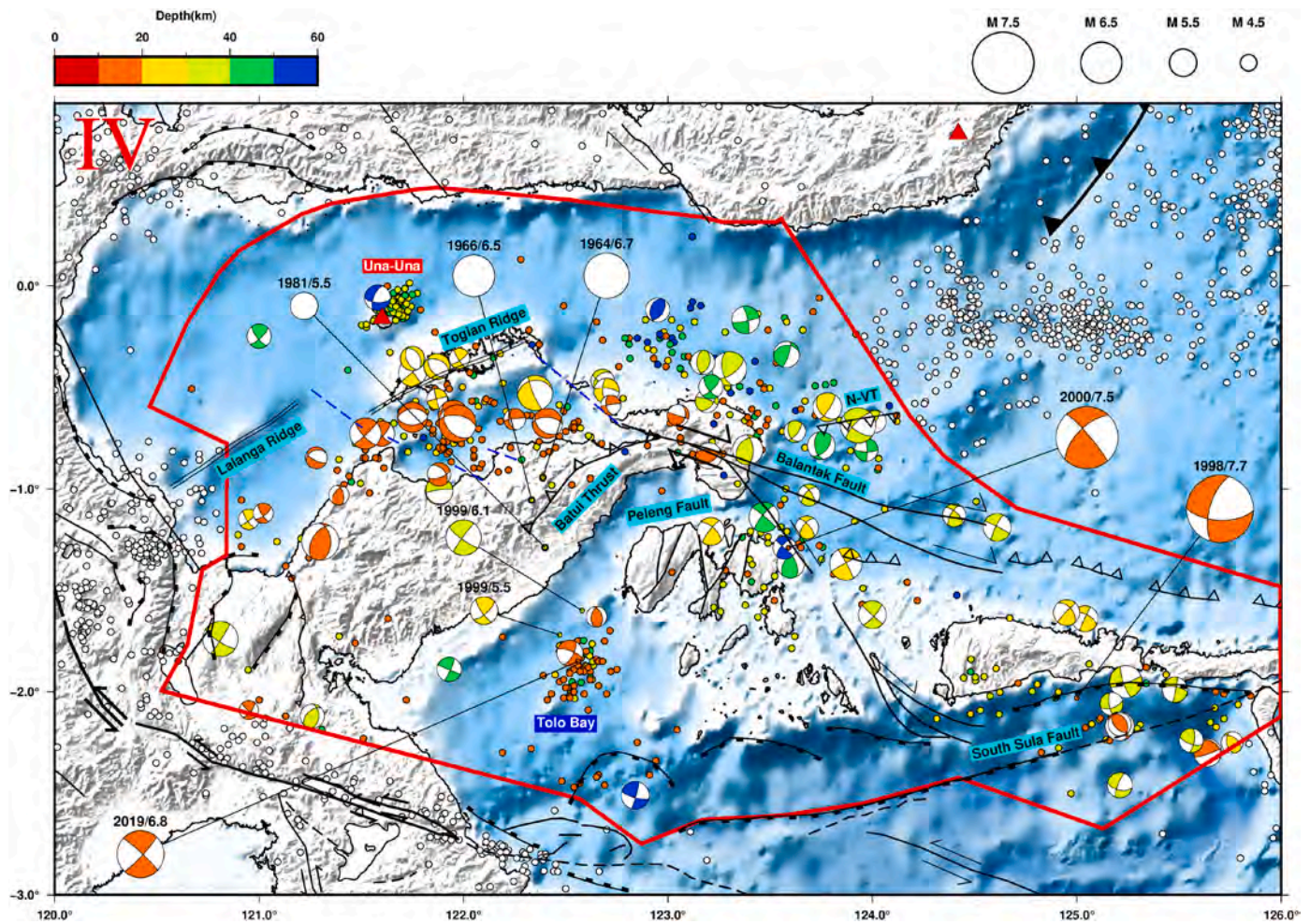


Fig. 7. Similar to Fig. 4 but for region IV. Earthquakes with $M_w \geq 6.5$ and in Tolo Bay zone are highlighted. The blue dashed line depicted possible faults (Pholbud et al., 2012). N-VT = North-Vergent Thrust. (For interpretation of the references to colour in this figure legend, the reader is referred to the web version of this article.)

extensional settings (Cottam et al., 2011). This is consistent with the occurrence of normal-type earthquakes and the low-velocity perturbation observed in the tomography model within this zone (B-B' profile in Fig. 9).

4.5. Region V (Fig. 8)

Seismotectonic sources in this region belonged to the Matano fault, Tolo thrust, Buton thrust, Kolaka fault, Lawanopo fault, Hamilton fault, and sporadic patterns off the coast of the Southeast Arm that might be related to the fault zones in the North Banda Sea. Along the Matano fault, seismicity patterns and the type of earthquake focal mechanisms reveal left-lateral strike-slip motions with a WNW-ESE trend, consistent with stream offsets of the fault (Hamilton, 1979). The 1980 Mw 6.1 and 2011 Mw 6.1 earthquakes are the two largest, accommodating the ~ 7 mm/yr slip rates (Rahmadani et al., 2022). The eastern edge of the Matano fault was interpreted to link with the arcuated Tolo thrust (Silver et al., 1983b; Hirschberger et al., 2005; Titu-Eki and Hall, 2020). The Tolo thrust was considered a possible future subduction zone (Hall, 2018), despite exhibiting a low level of seismicity with a few thrust mechanisms correlated to the trench. This zone also displayed clustered normal-type earthquakes with a striking perpendicular to the trench, which might be due to the Banda slab rollback.

The Buton thrust to the south exhibits low level of seismic activity as well, with a few thrust-type events near this fault's southern end off the coast. In the Southeast Arm, the seismicity related to the Kolaka strike-

slip fault only lay near its center with the normal-type earthquake, consistent with the study from Watkinson and Hall (2017), which found that the downthrown side existed to the south of this area. Seismic activity on the Lawanopo fault was low as well except for the 1980 Mw 6.1 near the center with dominantly normal type that might occur in the extensional step-over or pull-apart basin area (Watkinson and Hall, 2017). The Lawanopo fault's eastern continuation was connected to the Hamilton fault off the coast (Titu-Eki and Hall, 2020). The 2011 Mw 6.1 earthquake occurred at the junction of the two faults with a left-lateral strike-slip motion.

The Tamponas Fault Zone (TFZ) in the North Banda Sea Basin hosts the largest earthquake in the region, which occurred on October 19, 2001, with a magnitude of 7.5. This earthquake had a strike-slip mechanism near the western segment of the TFZ. While the event might have been triggered by the offshore continuation of the Lawanopo fault (Yeats, 2012), the centroid location and the distribution of aftershocks trending in a north-south direction suggest that the fault plane is likely the western segment of the TFZ. The latter possibility would require the reactivation of the TFZ's western segment from a left-lateral to a right-lateral strike-slip fault.

5. Discussions

Since the available period of the ISC-EHB catalog is between 1964 and 2019, we adopted data from the BMKG catalog to cover the period between 2020 and July 2022. Although there is a difference in the

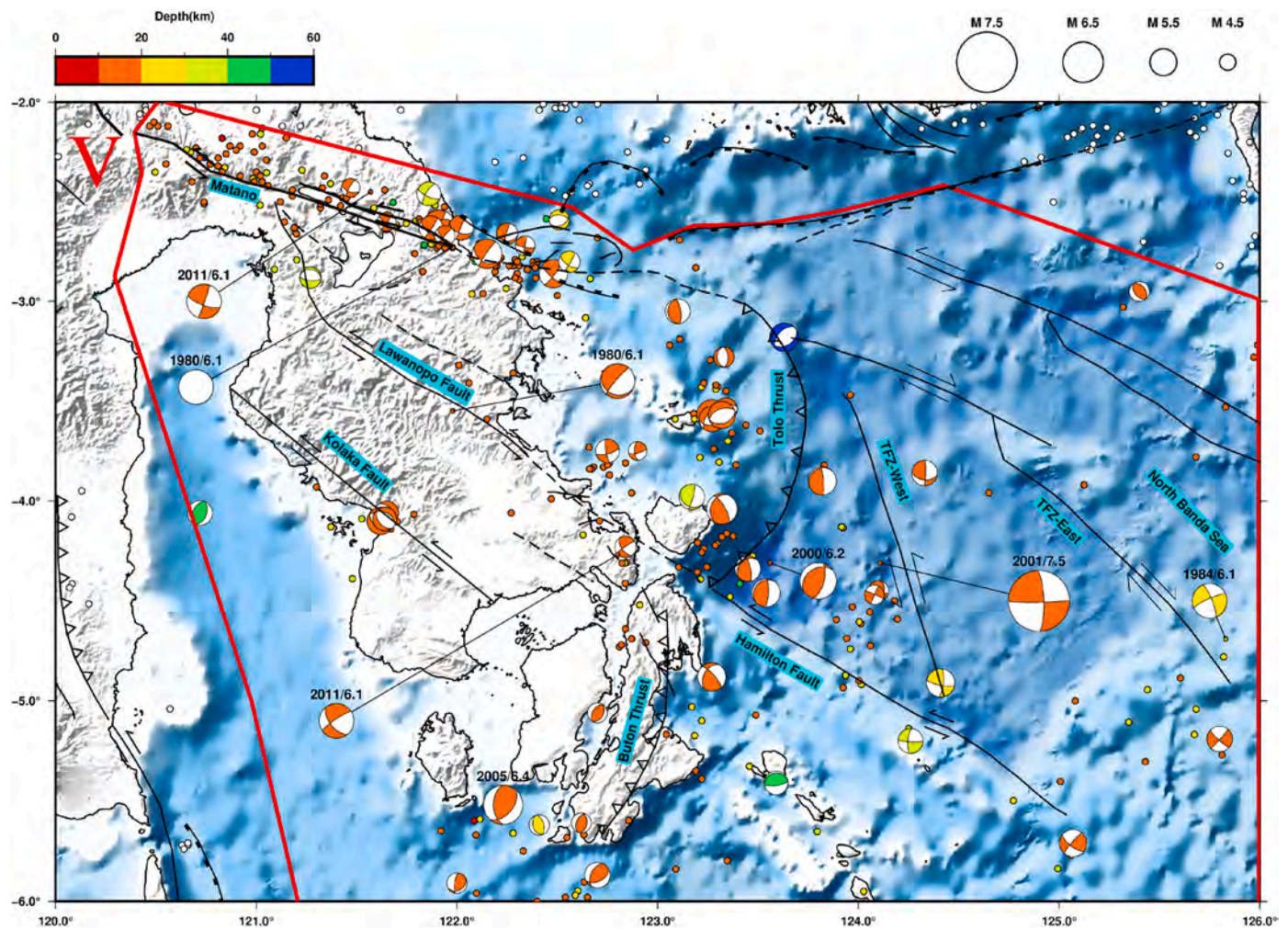


Fig. 8. Similar to Fig. 4 but for region V. Earthquakes with $M_w \geq 6.0$ are highlighted.

completeness of magnitude (M_w 4.3 for ISC-EHB and M_w 3.8 for BMKG), missing earthquakes of small magnitude are not going to invalidate the results of this study. Large earthquakes are representative of the patterns of seismic moment release (the moment release of one M_w 5.0 event is equivalent to that of 900 M_w 5.3 events). We justify this claim by including events with magnitudes less than M_w 4.3 between 2010 and 2019 and magnitudes less than M_w 3.8 between 2020 and 2022 from the BMKG catalog (Fig. S4).

The latest Miocene collision (~ 5 Ma) between the Banggai-Sula microcontinent and the East Arm of Sulawesi greatly impacted the deformation and stress patterns in and around Sulawesi Island. This impact is evident in the complex seismicity patterns and diverse earthquake mechanisms, providing valuable insights into the region's tectonic processes. For instance, in Region IV (Fig. 7), strike-slip earthquakes predominantly occur along the Balantak, Peleng, and South Sula faults. Additionally, relative motion between the Lalanga and Togian ridges may contribute to the strike-slip earthquakes near these two ridges. Thrust earthquakes are primarily associated with the Batui Thrust and the North-Vergent thrust, with the relative motion between these structures potentially contributing to the strike-slip earthquakes situated between them. Normal-type earthquakes are attributed to the extensional behavior of the Tojo Una-Una volcano, Lalanga Ridge, and Togian Ridge, supported by the presence of a low-velocity zone in this region (Fig. 9).

The latest Miocene collision also led to the clockwise and counter-clockwise rotation of the Northern and Southern blocks, respectively (Walpersdorf et al., 1998a, 1998b; Socquet et al., 2006). This relative

motion facilitated the development of several strike-slip faults in Sulawesi Island, including the formation of the Makassar Strait fault (Socquet et al., 2006; Jaya, 2014), as indicated by the seismicity distributions and focal mechanisms aligning with the active fault.

Various studies, including geodetic (Walpersdorf et al., 1998a, 1998b; Socquet et al., 2006), paleomagnetic (Otofuji et al., 1981; Surmont et al., 1994), geological (Silver et al., 1983b; Kopp et al., 1999), and seismic deformation analyses (Beaudouin et al., 2003) consistently report a westward increase in convergence rate along the North Sulawesi Trench (NST), ranging from 13 to 65 mm/yr. Recent numerical study (Dong et al., 2022) suggests that the latest Miocene collision provided an external force to induce subduction of the Celebes Sea initially, followed by spontaneous trench retreat of slab rollback due to the negative buoyancy of the subducting oceanic lithosphere. The presence of the Sangihe slab to the east restricts upper mantle space for Celebes Sea subduction and results in an easterly reduction of trench retreats, which in turn facilitates the clockwise rotation of the North Arm.

However, our investigation revealed that interplate (thrust) earthquake seismicity was notably low near the center of the trench (the purple dashed square in Fig. 4) compared to the east and west sides, where some large interplate earthquakes with $M_w \geq 6.5$ had occurred (Highlighted events in Fig. 4). Historical earthquake data (ISC-Bulletin, USGS, BMKG catalog) also show a lack of large earthquakes ($M \geq 6.5$) in this zone. This observation aligns with the rupture asperity of earthquakes with $M_w \geq 7.3$ (gray-colored area in Fig. 4), showing no rupture in this low-seismicity zone. Whether the seismic gap represents low-

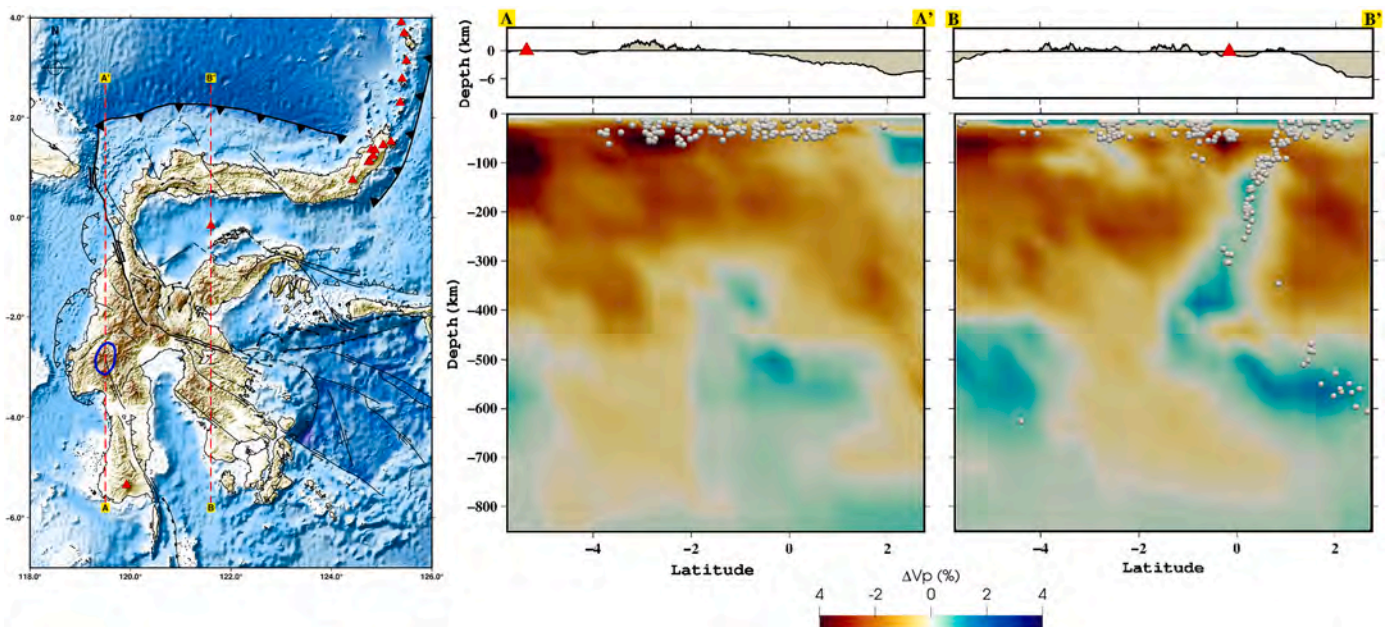


Fig. 9. The seismic tomography model of Sulawesi. The tomography data is the UU-P07 model (Amaru, 2007; Hall and Spakman, 2015). The maps show two vertical cross-sections of seismicity distributions (white dots) and P-wave velocity perturbations (colour-keyed), with each profile having a 50 km width on both sides. The red triangles are the volcanoes. The upper panel on each profile represents topography/bathymetry. The inset map displays the locations of the two profiles. The blue ellipse represent the Mamasa zone, while the red triangle in profile B-B' is the Una-Una volcano zone. Noted that these two zones are identified as the zone with low-velocity perturbation. (For interpretation of the references to colour in this figure legend, the reader is referred to the web version of this article.)

coupling zone [e.g., the Shumagin Gap in the Alaska-Aleutian subduction zone (Herman and Furlong, 2021)], aseismic behavior by slow-slip events [e.g., the Guerrero seismic gap in the Middle American Trench (Gualandi et al., 2017)], or a potential location of future large earthquake awaits the results of future geodetic studies.

Another significant consequence of the late Miocene collision is the emergence of the left-lateral Palu-Koro fault (Villeneuve et al., 2001; Bellier et al., 2006). While Hidayati et al. (2018) suggest a connection between the Palu-Koro and the fault near the Northeast Borneo, recent observations (Tiranda and Hall, 2024) revealed that the Palu-Koro fault is linked to the North Sulawesi Trench (NST) instead, with no evidence suggesting its extension into northeast Borneo. Furthermore, our seismicity analysis showed that the northernmost segment exhibits significantly lower seismicity compared to other sections along the Palu-Koro fault. This might be attributed to the location of this segment beyond the radius of high relative motion between the Makassar Block and the North Sula Block (Fig. 1b), implying that the influence of block interactions on the Palu-Koro fault weakens towards its northernmost extent, potentially contributing to the observed low seismicity.

Regarding the segment on land, present-day seismicity shows that the Palu-Koro fault in Region II is classified as a high slip rate (32–45 mm/yr) fault with historically low seismicity (Bellier et al., 2001). The occurrence of the 2018 Mw 7.6 Palu earthquake on 28th September not only filled the seismic gap of the Palu-Koro fault but also potentially triggered an overall increase in seismic activity in Sulawesi, particularly within six specific regions (Fig. 10; Fig. S5). The selection of these regions focused on areas that exhibited a significant increase in both the cumulative number of earthquakes and the cumulative seismic moment release following the 2018 Palu earthquake. Overall, these regions were previously seismically quiet before the 2018 Palu earthquake. We excluded areas close to the North Sulawesi subduction zone, as this region is already known to be tectonically active. To investigate the temporal and spatial scope of triggering, we analyzed the cumulative number and seismic moment of earthquakes as a function of time (year) for each region. The number counts events greater than Mw 4.3 between 1964 and the present day. We list the results for each region in

chronological order.

(1) The Mamasa zone swarm first commenced on November 2nd, 2018, and lasted for about a month or longer, resulting in an increasing number of 11 seismic events and a seismic moment release of 1.21×10^{25} dyne-cm/s (shown as [11 events, 1.21×10^{25} dyne-cm]). Swarm activity has calmed down since 2019 and continues to remain subdued (Fig. 10b; Fig. S5b). (2) After the Palu earthquake, the Tolo Bay zone experienced a significant increase in seismic activity [21 events, 1.96×10^{26} dyne-cm] from April to June 2019, with the largest one being the Mw 6.8 earthquake on April 12th, 2019. Prior to the Palu earthquake, the Tolo Bay zone had been relatively quiescent in terms of Mw ≥ 4.3 events, except for an Mw 6.1 earthquake followed by an Mw 5.5 earthquake in August 1999 (Fig. 10c; Fig. S5c). (3) The area east of MST central exhibited a low level of seismicity during the periods prior to the Palu earthquake. However, there was a significant jump in seismicity [8 events, 2.49×10^{24} dyne-cm] during the 2020 period, followed by a period of quiescence that continues up to the present (Fig. 10d; Fig. S5d). (4) In the MST-Mamuju zone, only 9 earthquakes with Mw ≥ 4.3 are recorded in our dataset, concentrating in 1984 and 2021. While the unrest in 1984 collectively released 1.28×10^{26} dyne-cm of the total moment through an Mw 6.7 and an Mw 5.5 earthquake, the activity in 2021 was the Mamuju-Majene sequence (Supendi et al., 2021; Meilano et al., 2022), which accounted for the 3.69×10^{25} dyne-cm moment release (Fig. 10e; Fig. S5e). (5) In the vicinity of the East Arm-Togian ridge zone, seismic activity remains consistently active due to a complex tectonic environment, steadily increasing the cumulative number by an average of 1–4 events per year. Nevertheless, anomalously high activity was observed in 2021 [10 events, 2.88×10^{25} dyne-cm], with the latter primarily attributed to the 2021 Tojo Una-Una earthquake (Fig. 10f; Fig. S5f). Finally, the Matano fault, serving as the southern extension of the Palu-Koro fault, exhibited an increase in seismic activity in 2020 (Fig. 10g; Fig. S5g). However, the seismic events occurring in 2017, prior to the Palu earthquake, were even more remarkable. Understanding the interaction and evolution of earthquakes on both the Palu-Koro and Matano faults over time is a topic that warrants further investigation.

We investigated the spatial distributions of the five seismic regions

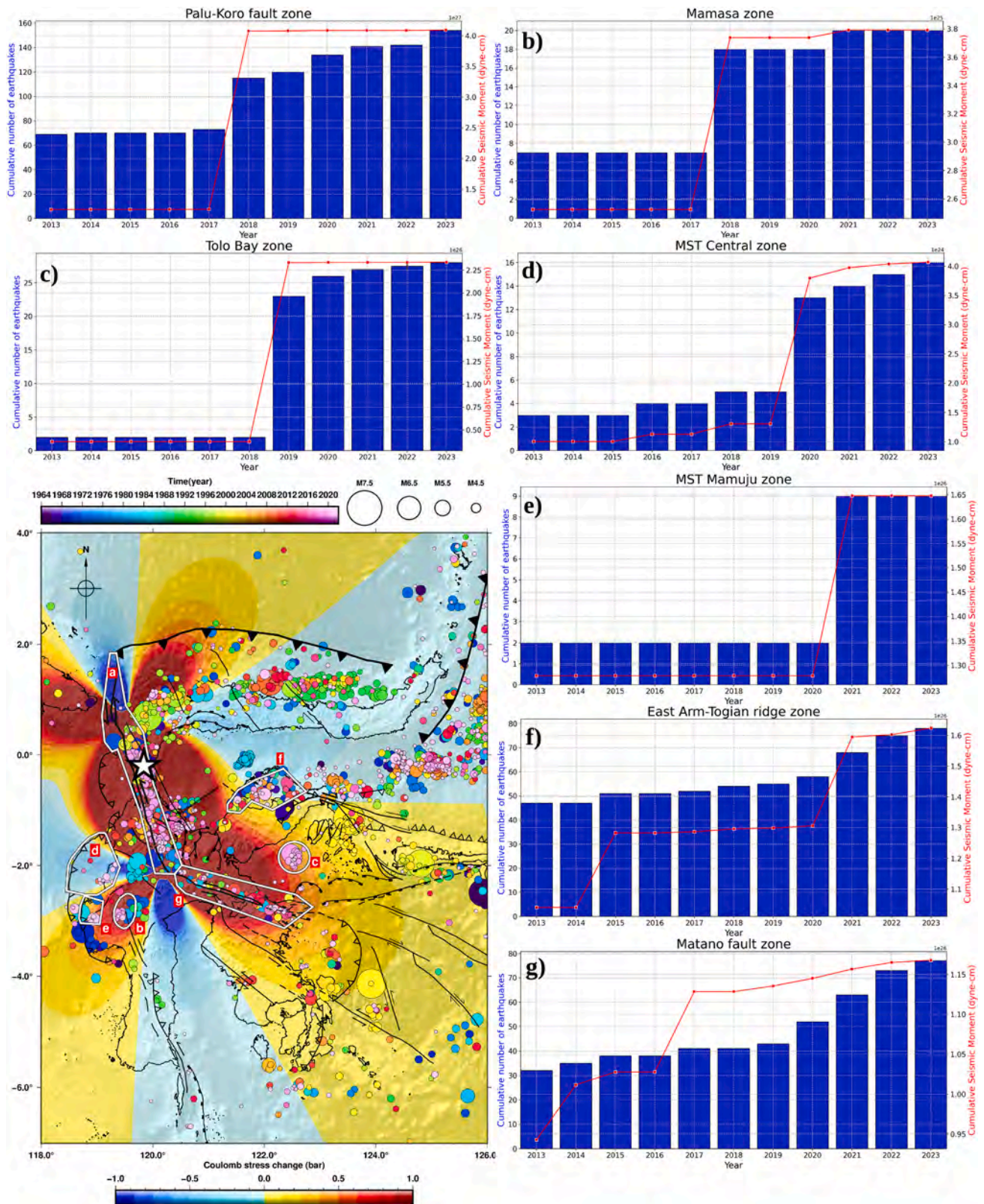


Fig. 10. The cumulative number of earthquakes (blue bar) and cumulative seismic moment (red line) as a function of the time (year) in the 7 specific zones with ± 5 years relative to the 2018 Palu earthquake. For the longer time span, see Fig. S4. a = Palu-Koro fault zone, b = Mamasa zone, c = Tolo Bay zone, d = MST Central zone, e = MST mamuju zone, f = East Arm-Togian ridge zone, g = Matano fault zone. The inset map displays the location of specific zones (white coherence shapes) with the distribution of seismicity ($M_w \geq 4.3$). The dots are scaled with magnitudes and colour-keyed in time (year). The blue-red contour is the Coulomb stress changes at 10 km depth due to the 2018 Mw 7.6 Palu earthquake (Wibowo et al., 2020). The white star is the mainshock of Palu earthquake. The tectonic structures are identical to Fig. 1c. (For interpretation of the references to colour in this figure legend, the reader is referred to the web version of this article.)

that experienced increased seismic activity due to Coulomb stress changes induced by the Palu earthquake (Wibowo et al., 2020). All these regions are situated within the zone of increasing Coulomb stress, except for the area east of MST central. This suggests that the Palu earthquake may have indirectly influenced seismicity in this region, potentially by triggering activity on nearby faults. Overall, the results suggest that the Palu earthquake indeed played a role in triggering seismic activity throughout Sulawesi as a whole.

6. Conclusion

In this study, we investigate the distributions of shallow earthquakes (< 60 km) based on the ISC-EHB and BMKG catalogs, as well as the focal mechanisms based on the GCMT catalog, to study the seismotectonics of Sulawesi. The conclusions are as follows:

6.1. Region I

Along NST, the Celebes Sea subduction zone exhibits predominantly interplate thrust earthquakes dipping shallowly to the south. The seismic gap near the center of the North Arm of Sulawesi (longitude $\sim 121^{\circ}$ – 121.7° E) could be related to either seismic gap or aseismic slip. On the other hand, the potential for a large earthquake associated with the Gorontalo fault cannot be ruled out.

6.2. Region II

The occurrence of the 2018 Mw 7.6 Palu earthquake on 28th September not only filled the gap of seismic deficiency of the Palu-Koro fault but also triggered overall seismic activity in Sulawesi. The segment of the Palu-Koro fault offshore northwest Sulawesi exhibits a low level of seismicity, possibly due to being beyond the high relative motion of the MKB-NSB.

6.3. Region III

Seismic moment release is driven by, in order of activity, convergence across the Makassar Strait Thrust, swarms related to magmatic activity in the Mamasa zone, and those of the East Walane Fault. Among the five segments of MST, MST Mamuju and MST Somba, experienced the highest magnitudes of 6.7 and 7.1, respectively.

6.4. Region IV

This region can be characterized as the most complex region in Sulawesi, as reflected by the presence of various active faults, extensional settings, volcanoes, and fault reactivation, including the largest earthquake (Mw 7.7) in our study area. The Tolo Bay earthquake in this region might be related to the southwest off-coast continuation of the Peleng fault, which was previously unidentified.

6.5. Region V

Seismotectonic sources in this region belong to the Matano fault, Tolo thrust, Buton thrust, Kolaka fault, Lawanopo fault, Hamilton fault, and sporadic patterns related to the fault zones in the North Banda Sea (the 2001 Mw 7.5 on 19 Oct.). We propose that the 2001 event likely ruptured the western segment of the Tamponas Fault Zone, which would require the reactivation of its western segment from a left-lateral to a right-lateral strike-slip fault.

CRediT authorship contribution statement

Yopi Serhalawan: Writing – original draft, Visualization, Methodology, Investigation. **Po-Fei Chen:** Writing – review & editing, Supervision, Project administration, Methodology, Investigation, Funding

acquisition, Conceptualization.

Declaration of competing interest

The authors declare that they have no known competing financial interests or personal relationships that could have appeared to influence the work reported in this paper.

Data availability

The seismicity data were obtained from the ISC-EHB catalog available at <http://www.isc.ac.uk/isc-ehb/search/catalogue/> (Engdahl et al., 2020) and the BMKG catalog. The focal mechanisms data were retrieved from the Global CMT catalog which, can be accessed at <https://www.globalcmt.org/>; (Dziewonski et al., 1981; Ekström et al., 2012). The tomography data used in this study is the UU-P07 model downloaded at <https://www.atlas-of-the-underworld.org/downloads/> (UU-P07 model; Amaru, 2017; Hall and Spakman, 2015).

Acknowledgment

We are grateful to the two anomalous reviewers for their constructive opinions. We sincerely thank Dr. Dimas S. J. Sianipar for his help in preparing the data and fruitful discussions. Additionally, we extend our thanks to Adhi Wibowo, S.T., M.Sc for providing the data regarding the Coulomb stress change resulting from the 2018 Palu earthquake. This work was supported by the Taiwan Earthquake Research Center (TEC) funded through the National Science and Technology Council (NSTC) of Taiwan with Grant Number NSTC 112-2116-M-008-003. The TEC contribution number for this article is 00189. Some figures were prepared with the Generic Mapping Tools Version 6 (Wessel et al., 2019).

Appendix A. Supplementary data

Supplementary data to this article can be found online at <https://doi.org/10.1016/j.tecto.2024.230366>.

References

- Advokaat, E.L., Hall, R., White, L.T., Watkinson, I.M., Rudyawan, A., BouDagher-Fadel, M.K., 2017. Miocene to recent extension in NW Sulawesi, Indonesia. *J. Asian Earth Sci.* 147, 378–401. <https://doi.org/10.1016/j.jseae.2017.07.023>.
- Amaru, M.L.L. Global Travel Time Tomography with 3-D Reference Models (Doctoral dissertation). Retrieved from Utrecht University Repository. <https://dspace.library.uu.nl/handle/1874/19338>.
- Beaudouin, T., Bellier, O., Sebrier, M., 2003. Present-day stress and deformation field within the Sulawesi Island area (Indonesia) : geodynamic implications. *Bulletin De La Société Géologique De France* 174 (3), 305–317. <https://doi.org/10.2113/174.3.305>.
- Bellier, O., Sebrier, M., Beaudouin, T., Villeneuve, M., Braucher, R., Bourles, D., Siame, L., Putranto, E., Pratomo, I., 2001. High slip rate for a low seismicity along the Palu-Koro active fault in Central Sulawesi (Indonesia). *Terra Nova* 13 (6), 463–470. <https://doi.org/10.1046/j.1365-3121.2001.00382.x>.
- Bellier, O., Sébrier, M., Seward, D., Beaudouin, T., Villeneuve, M., Putranto, E., 2006. Fission track and fault kinematics analyses for new insight into the Late Cenozoic tectonic regime changes in West-Central Sulawesi (Indonesia). *Tectonophysics* 413 (3–4), 201–220. <https://doi.org/10.1016/j.tecto.2005.10.036>.
- Bratt, S.R., Bache, T.C., 1988. Locating events with a sparse network of regional arrays. *Bull. Seismol. Soc. Am.* 78 (2), 780–798. <https://doi.org/10.1785/BSSA0780020780>.
- Camplin, D.J., Hall, R., 2014. Neogene history of Bone Gulf, Sulawesi, Indonesia. *Mar. Pet. Geol.* 57, 88–108. <https://doi.org/10.1016/j.marpetgeo.2014.04.014>.
- Chen, P.S., Olaverre, E.A., Wang, C., Bautista, B.C., Solidum, R.U., Liang, W., 2015. Seismotectonics of Mindoro, Philippines. *Tectonophysics* 640–641, 70–79. <https://doi.org/10.1016/j.tecto.2014.11.023>.
- Cottam, M.A., Hall, R., Forster, M.A., Boudagher-Fadel, M.K., 2011. Basement character and basin formation in Gorontalo Bay, Sulawesi, Indonesia: new observations from the Togan Islands. *Geol. Soc. Lond. Spec. Publ.* 355 (1), 177–202. <https://doi.org/10.1144/sp355.9>.
- Daniarsyad, G., Sianipar, D., Heryandoko, N., Priyobudi, P., 2021. Source mechanism of the 29 May 2017 Mw 6.6 Poso (Sulawesi, Indonesia) earthquake and its seismotectonic implication. *Pure Appl. Geophys.* 178 (8), 2807–2819. <https://doi.org/10.1007/s00024-021-02779-y>.

- DeMets, C., Gordon, R.G., Argus, D.F., 2010. Geologically current plate motions. *Geophys. J. Inter.* 181 (1), 1–80. <https://doi.org/10.1111/j.1365-246x.2009.04491.x>.
- Dong, M., Lü, C., Zhang, J., Hao, T., 2022. Downgoing Plate-Buoyancy driven retreat of North Sulawesi Trench: transition of a passive margin into a subduction zone. *Geophys. Res. Lett.* 49 (23) <https://doi.org/10.1029/2022gl101130>.
- Dziwowski, A.M., Chou, T.A., Woodhouse, J.H., 1981. Determination of earthquake source parameters from waveform data for studies of global and regional seismicity. *J. Geophys. Res. Solid Earth* 86 (B4), 2825–2852. <https://doi.org/10.1029/jb086ib04p02825>.
- Ekström, G., Nettles, M., Dziwowski, A., 2012. The global CMT project 2004–2010: Centroid-moment tensors for 13,017 earthquakes. *Phys. Earth Planet. Inter.* 200–201, 1–9. <https://doi.org/10.1016/j.pepi.2012.04.002>.
- Engdahl, E.R., Van Der Hilst, R.D., Buland, R., 1998. Global teleseismic earthquake relocation with improved travel times and procedures for depth determination. *Bull. Seismol. Soc. Am.* 88 (3), 722–743. <https://doi.org/10.1785/bssa0880030722>.
- Engdahl, E.R., Di Giacomo, D., Sakarya, B., Gkaraklaou, C.G., Harris, J., Storchak, D.A., 2020. ISC-EHB 1964–2016, an improved data set for studies of Earth structure and global seismicity. *Earth Space Sci.* 7 (1), e2019EA000897 <https://doi.org/10.1029/2019ea000897>.
- Fortuin, A., De Smet, M., Hadiwasastira, S., Van Marle, L., Troelstra, S., Tjokrosapetro, S., 1990. Late Cenozoic sedimentary and tectonic history of south Buton, Indonesia. *J. Southeast Asian Earth Sci.* 4 (2), 107–124. [https://doi.org/10.1016/0743-9547\(90\)90010-b](https://doi.org/10.1016/0743-9547(90)90010-b).
- Frohlich, C.A., Apperson, K.D., 1992. Earthquake focal mechanisms, moment tensors, and the consistency of seismic activity near plate boundaries. *Tectonics* 11 (2), 279–296. <https://doi.org/10.1029/91tc02888>.
- Greenfield, T., Copley, A.C., Caplan, C., Supendi, P., Widiyantoro, S., Rawlinson, N., 2021. Crustal deformation and fault strength of the Sulawesi subduction zone. *Tectonics* 40 (3). <https://doi.org/10.1029/2020tc006573>.
- Gualandi, A., Perfettini, H., Radiguet, M., Cotte, N., Kostoglodov, V., 2017. GPS deformation related to the M_w 7.3, 2014, Papanoa earthquake (Mexico) reveals the aseismic behavior of the Guerrero seismic gap. *Geophys. Res. Lett.* 44, 6039–6047. <https://doi.org/10.1002/2017gl072913>.
- Hall, R., 1996. Reconstructing Cenozoic SE Asia. *Geol. Soc. Lond. Spec. Publ.* 106 (1), 153–184. <https://doi.org/10.1144/gsl.sp.1996.106.01.11>.
- Hall, R., 2002. Cenozoic geological and plate tectonic evolution of SE Asia and the SW Pacific: computer-based reconstructions, model and animations. *J. Asian Earth Sci.* 20 (4), 353–431. [https://doi.org/10.1016/s1367-9120\(01\)00069-4](https://doi.org/10.1016/s1367-9120(01)00069-4).
- Hall, R., 2012. Late Jurassic–Cenozoic reconstructions of the Indonesian region and the Indian Ocean. *Tectonophysics* 570–571, 1–41. <https://doi.org/10.1016/j.tecto.2012.04.021>.
- Hall, R., 2018. The subduction initiation stage of the Wilson cycle. *Geol. Soc. Lond. Spec. Publ.* 470 (1), 415–437. <https://doi.org/10.1144/sp470.3>.
- Hall, R., Sevastjanova, I., 2012. Australian crust in Indonesia. *Aust. J. Earth Sci.* 59 (6), 827–844. <https://doi.org/10.1080/08120099.2012.692335>.
- Hall, R., Spakman, W., 2015. Mantle structure and tectonic history of SE Asia. *Tectonophysics* 658, 14–45. <https://doi.org/10.1016/j.tecto.2015.07.003>.
- Hall, R., Wilson, M., 2000. Neogene sutures in eastern Indonesia. *J. Asian Earth Sci.* 18 (6), 781–808. [https://doi.org/10.1016/s1367-9120\(00\)00040-7](https://doi.org/10.1016/s1367-9120(00)00040-7).
- Hamilton, W.B., 1979. *Tectonics of the Indonesian Region*. Professional Paper, 1078. U.S. Geological Survey, Washington, DC. <https://doi.org/10.3133/pp1078>.
- Hayes, G.P., 2017. The finite, kinematic rupture properties of great-sized earthquakes since 1990. *Earth Planet. Sci. Lett.* 468, 94–100. <https://doi.org/10.1016/j.epsl.2017.04.003>.
- Hayes, G.P., Moore, G.L., Portner, D.E., Hearne, M., Flamme, H., Furtney, M., Smoczyk, G.M., 2018. Slab2, a comprehensive subduction zone geometry model. *Science* 362 (6410), 58–61. <https://doi.org/10.1126/science.aat4723>.
- He, L., Feng, G., Li, Z., Feng, Z., Gao, H., Wu, X., 2019. Source parameters and slip distribution of the 2018 M 7.5 Palu, Indonesia earthquake estimated from space-based geodesy. *Tectonophysics* 772, 228216. <https://doi.org/10.1016/j.tecto.2019.228216>.
- Herman, M.W., Furlong, K.P., 2021. Triggering an unexpected earthquake in an uncoupled subduction zone. *Sci. Adv.* 7 (13) <https://doi.org/10.1126/sciadv.abf7590>.
- Hidayati, S., Guritno, E., Argenton, A., Ziza, W., Del Campana, I., 2018. Re-visited structural framework of the Tarakan Sub-Basin Northeast Kalimantan – Indonesia. In: *Proc. Indon. Petrol. Assoc.*, 31st Ann. Conv.. <https://doi.org/10.29118/ipa.1717.07.g.109>.
- Hinschberger, F., Malod, J.A., Réhault, J.P., Dymant, J., Honthaaas, C., Villeneuve, M., Burhanuddin, S., 2000. Origine et évolution du bassin Nord-Banda (Indonésie): apport des données magnétiques. *C. R. Acad. Sci. Ser. IIA Earth Planet. Sci.* 331 (7), 507–514. [https://doi.org/10.1016/s1251-8050\(00\)01438-5](https://doi.org/10.1016/s1251-8050(00)01438-5).
- Hinschberger, F., Malod, J.A., Dymant, J., Honthaaas, C., Réhault, J.P., Burhanuddin, S., 2001. Magnetic lineations constraints for the back-arc opening of the Late Neogene South Banda Basin (Eastern Indonesia). *Tectonophysics* 333 (1–2), 47–59. [https://doi.org/10.1016/s0040-1951\(00\)00266-3](https://doi.org/10.1016/s0040-1951(00)00266-3).
- Hinschberger, F., Malod, J.A., Réhault, J.P., Burhanuddin, S., 2003. Contribution of bathymetry and geomorphology to the geodynamics of the East Indonesian Seas. *Bulletin De La Société Géologique De France* 174 (6), 545–560. <https://doi.org/10.2113/174.6.545>.
- Hinschberger, F., Malod, J.A., Réhault, J.P., Villeneuve, M., Royer, J.Y., Burhanuddin, S., 2005. Late Cenozoic geodynamic evolution of eastern Indonesia. *Tectonophysics* 404 (1–2), 91–118. <https://doi.org/10.1016/j.tecto.2005.05.005>.
- Hutchings, S.J., Mooney, W.D., 2021. The Seismicity of Indonesia and Tectonic Implications. *Geochem. Geophys. Geosyst.* 22 (9), e2021GC009812 <https://doi.org/10.1029/2021gc009812>.
- Irsyam, M., Cummins, P.R., Asrurifak, M., Faizal, L., Natawidjaja, D.H., Widiyantoro, S., Meilano, I., Triyoso, W., Rudiyanto, A., Hidayati, S., Ridwan, M., Hanifa, N.R., Syahbana, A.A., 2020. Development of the 2017 national seismic hazard maps of Indonesia. *Earthquake Spectra* 36 (1_suppl), 112–136. <https://doi.org/10.1177/8755293020951206>.
- Jaya, A., Tectonic Evolution of South Sulawesi, Indonesia: Reconstructed by Analysis of Deformation Structures (Doctoral dissertation). Retrieved from Akita University Institutional Repository System. <https://air.repo.nii.ac.jp>. Akita University, Akita.
- Kopp, C., Flueh, E., Neben, S., 1999. Rupture and accretion of the Celebes Sea crust related to the North–Sulawesi subduction: combined interpretation of reflection and refraction seismic measurements. *J. Geodyn.* 27 (3), 309–325. [https://doi.org/10.1016/s0264-3707\(98\)00004-0](https://doi.org/10.1016/s0264-3707(98)00004-0).
- Kouali, A., Susilo, S., McClusky, S., Meilano, I., Cummins, P., Tregoning, P., Lister, G., Efendi, J., Syaifi, M.A., 2016. Crustal strain partitioning and the associated earthquake hazard in the eastern Sunda-Banda Arc. *Geophys. Res. Lett.* 43 (5), 1943–1949. <https://doi.org/10.1002/2016gl067941>.
- Liu, C., Shi, Y., 2021. Space-Time stress variations on the Palu-Koro fault impacting the 2018 MW 7.5 Palu earthquake and its seismic hazards. *Geochem. Geophys. Geosyst.* 22 (5) <https://doi.org/10.1029/2020gc009552>.
- Liu, C., Shi, Y., 2022. The role of fault interaction in earthquake migration in Central Sulawesi, Indonesia. *Tectonophysics* 839, 229530. <https://doi.org/10.1016/j.tecto.2022.229530>.
- Meilano, I., Salman, R., Susilo, S., Shiddiqi, H.A., Supendi, P., Lythgoe, K., Tay, C., Bradley, K., Rahmadani, S., Kristyawan, S., Yun, S., 2022. The 2021MW 6.2 Mamuju West Sulawesi, Indonesia earthquake: partial rupture of the Makassar Strait thrust. *Geophys. J. Int.* 233 (3), 1694–1707. <https://doi.org/10.1093/gji/ggac512>.
- Natawidjaja, D.H., Daryono, M.R., 2015. The Lawanopo Fault, Central Sulawesi, East Indonesia. *AIP Conf. Proc.* 1658 (1), 030001 <https://doi.org/10.1063/1.4915009>.
- Natawidjaja, D.H., Daryono, M.R., Prasetya, G., Udrek, Liu, Hananto, N.D., Kongko, W., Triyoso, W., Puji, A.R., Meilano, I., Gunawan, E., Supendi, P., Pamumpuni, A., Irsyam, M., Faizal, L., Hidayati, S., Sapiie, B., Kusuma, M.A., Tawil, S., 2020. The 2018 Mw7.5 Palu ‘supershear’ earthquake ruptures geological fault’s multi-segment separated by large bends: results from integrating field measurements, LiDAR, swath bathymetry, and seismic-reflection data. *Geophys. J. Int.* <https://doi.org/10.1093/gji/ggaa498>.
- Nugraha, A.M.S., Hall, R., BouDagher-Fadel, M., 2022. The Celebes Molasse: a revised Neogene stratigraphy for Sulawesi, Indonesia. *J. Asian Earth Sci.* 228, 105140 <https://doi.org/10.1016/j.jseas.2022.105140>.
- Otofuji, Y.I., Sasajima, S., Nishimura, S., Dharmas, A., Hehuwat, F., 1981. Paleomagnetic evidence for clockwise rotation of the northern arm of Sulawesi, Indonesia. *Earth Planet. Sci. Lett.* 54 (2), 272–280. [https://doi.org/10.1016/0012-821x\(81\)90010-8](https://doi.org/10.1016/0012-821x(81)90010-8).
- Parkinson, C.D., 1996. The origin and significance of metamorphosed tectonic blocks in mélanges: evidence from Sulawesi, Indonesia. *Terra Nova* 8 (4), 312–323. <https://doi.org/10.1111/j.1365-3121.1996.tb00564.x>.
- Parkinson, C., 1998. Emplacement of the East Sulawesi Ophiolite: evidence from subophiolite metamorphic rocks. *J. Asian Earth Sci.* 16 (1), 13–28. [https://doi.org/10.1016/s0743-9547\(97\)00039-1](https://doi.org/10.1016/s0743-9547(97)00039-1).
- Pholbud, P., Hall, R., Advokaat, E., Burgess, P.M., Rudyawan, A., 2012. A new interpretation of Gorontalo Bay, Sulawesi. In: *Indonesian Petroleum Association Proceedings 36th Annual Convention*, IPA 12-G-039, pp. 1–23.
- Polvé, M., Maury, R., Bellon, B., Rangin, C., Priadi, B., Yuwono, S., Joron, J., Atmadja, R., 1997. Magmatic evolution of Sulawesi (Indonesia): constraints on the Cenozoic geodynamic history of the Sundaland active margin. *Tectonophysics* 272 (1), 69–92. [https://doi.org/10.1016/s0040-1951\(96\)00276-4](https://doi.org/10.1016/s0040-1951(96)00276-4).
- Potsdam, H.C., 2008. The SeisComp Seismological Software Package [Software]. GFZ German Research Centre for Geosciences and Gempa GmbH. <https://doi.org/10.5880/GFZ.2.4.2020.003>.
- Rahmadani, S., Meilano, I., Susilo, S., Sarsito, D.A., Abidin, H.Z., Supendi, P., 2022. Geodetic observation of strain accumulation in the Banda Arc region. *Geomat. Nat. Haz. Risk* 13 (1), 2579–2596. <https://doi.org/10.1080/19475705.2022.2126799>.
- Scordilis, E.M., 2006. Empirical Global Relations Converting M S and m b to Moment Magnitude. *J. Seismol.* 10 (2), 225–236. <https://doi.org/10.1007/s10950-006-9012-4>.
- Siebert, L., Simkin, T., 2002. *Volcanoes of the World: An Illustrated Catalog of Holocene Volcanoes and their Eruptions [Dataset]*. Smithsonian Institution. www.volcano.si.edu/world.
- Silver, E.A., McCaffrey, R., Joyodiwiryo, Y., Stevens, S., 1983a. Ophiolite emplacement by collision between the Sula Platform and the Sulawesi Island Arc, Indonesia. *J. Geophys. Res. Solid Earth* 88 (B11), 9419–9435. <https://doi.org/10.1029/jb088ib11p09419>.
- Silver, E.A., McCaffrey, R., Smith, R.B., 1983b. Collision, rotation, and the initiation of subduction in the evolution of Sulawesi, Indonesia. *J. Geophys. Res. Solid Earth* 88 (B11), 9407–9418. <https://doi.org/10.1029/jb088ib11p09407>.
- Simandjuntak, T.O. *Sedimentology and Tectonics of the Collision Complex in the East Arm of Sulawesi, Indonesia (Doctoral dissertation)*. Retrieved from Royal Holloway Repository. <https://repository.royalholloway.ac.uk>.
- Socquet, A., Simons, W., Vigny, C., McCaffrey, R., Subarya, C., Sarsito, D., Ambrosius, B., Spakman, W., 2006. Microblock rotations and fault coupling in SE Asia triple junction (Sulawesi, Indonesia) from GPS and earthquake slip vector data. *J. Geophys. Res.* 111 (B8), B08409. <https://doi.org/10.1029/2005jb003963>.
- Song, T., Hao, T., Zhang, J., Cao, L., Dong, M., 2022. Numerical modeling of North Sulawesi subduction zone: Implications for the east–west differential evolution. *Tectonophysics* 822, 229172. <https://doi.org/10.1016/j.tecto.2021.229172>.

- Supendi, P., Nugraha, A.D., Widiyantoro, S., Abdullah, C.I., Puspito, N.T., Palgunadi, K. H., Daryono, D., Wiyono, S.H., 2019. Hypocenter relocation of the aftershocks of the Mw 7.5 Palu earthquake (September 28, 2018) and swarm earthquakes of Mamasa, Sulawesi, Indonesia, using the BMKG network data. *Geosci. Lett.* 6 (1), 18. <https://doi.org/10.1186/s40562-019-0148-9>.
- Supendi, P., Ramdhan, M., Priyobudi, Sianipar D., Wibowo, A., Gunawan, M.T., Rohadi, S., Riama, N.F., Daryono, Prayitno B.S., Murjaya, J., Karnawati, D., Meilano, I., Rawlinson, N., Widiyantoro, S., Nugraha, A.D., Marliyani, G.I., Palgunadi, K.H., Elsera, E.M., 2021. Foreshock–mainshock–aftershock sequence analysis of the 14 January 2021 (Mw 6.2) Mamuju–Majene (West Sulawesi, Indonesia) earthquake. *Earth Planets Space* 73 (1), 106. <https://doi.org/10.1186/s40623-021-01436-x>.
- Surmont, J., Laj, C., Kissel, C., Rangin, C., Bellon, H., Priadi, B., 1994. New paleomagnetic constraints on the Cenozoic tectonic evolution of the North Arm of Sulawesi, Indonesia. *Earth Planet. Sci. Lett.* 121 (3–4), 629–638. [https://doi.org/10.1016/0012-821x\(94\)90096-5](https://doi.org/10.1016/0012-821x(94)90096-5).
- Tiranda, H., Hall, R., 2024. Structural and Stratigraphic Development of Offshore NW Sulawesi, Indonesia. *EarthArxiv*. <https://doi.org/10.31223/x5wc89>.
- Titu-Eki, A., Hall, R., 2020. The significance of the Banda Sea: tectonic deformation review in Eastern Sulawesi. *Indonesian J. Geosci.* 7 (3), 291–303. <https://doi.org/10.17014/ijog.7.3.291-303>.
- Tozer, B., Sandwell, D.T., Smith, W.H.F., Olson, C., Beale, J.R., Wessel, P., 2019. Global Bathymetry and Topography at 15 arc Sec: SRTM15+. *Earth and Space Science* 6 (10), 1847–1864. <https://doi.org/10.1029/2019ea000658>.
- van Leeuwen, T.M., Muhardjo., 2005. Stratigraphy and tectonic setting of the cretaceous and Paleogene volcanic-sedimentary successions in Northwest Sulawesi, Indonesia: implications for the Cenozoic evolution of Western and Northern Sulawesi. *J. Asian Earth Sci.* 25 (3), 481–511. <https://doi.org/10.1016/j.jseas.2004.05.004>.
- van Leeuwen, T., Allen, C.M., Kadarusman, A., Elburg, M., Michael Palin, J., Muhardjo, Suwijanto, 2007. Petrologic, isotopic, and radiometric age constraints on the origin and tectonic history of the Malino Metamorphic complex, NW Sulawesi, Indonesia. *J. Asian Earth Sci.* 29 (5–6), 751–777. <https://doi.org/10.1016/j.jseas.2006.05.002>.
- van Leeuwen, T., Allen, C.M., Elburg, M., Massonne, H.J., Palin, J.M., Hennig, J., 2016. The Palu Metamorphic complex, NW Sulawesi, Indonesia: Origin and evolution of a young metamorphic terrane with links to Gondwana and Sundaland. *J. Asian Earth Sci.* 115, 133–152. <https://doi.org/10.1016/j.jseas.2015.09.025>.
- Villeneuve, M., Gunawan, W., Cornee, J.J., Vidal, O., 2001. Geology of the Central Sulawesi belt (eastern Indonesia): constraints for geodynamic models. *Int. J. Earth Sci.* 91 (3), 524–537. <https://doi.org/10.1007/s005310100228>.
- Walpersdorf, A., Rangin, C., Vigny, C., 1998a. GPS compared to long-term geologic motion of the north arm of Sulawesi. *Earth Planet. Sci. Lett.* 159 (1–2), 47–55. [https://doi.org/10.1016/s0012-821x\(98\)00056-9](https://doi.org/10.1016/s0012-821x(98)00056-9).
- Walpersdorf, A., Vigny, C., Manurung, P., Subarya, C., Sutisna, S., 1998b. Determining the Sula block kinematics in the triple junction area in Indonesia by GPS. *Geophys. J. Int.* 135 (2), 351–361. <https://doi.org/10.1046/j.1365-246x.1998.00641.x>.
- Wang, S., Xu, C., Xu, W., Yin, Z., Wen, Y., Jiang, G., 2018. The 2017 Mw 6.6 Poso earthquake: implications for extrusion tectonics in Central Sulawesi. *Seismol. Res. Lett.* 90 (2A), 649–658. <https://doi.org/10.1785/0220180211>.
- Watkinson, I.M., Hall, R., 2017. Fault systems of the eastern Indonesian triple junction: evaluation of Quaternary activity and implications for seismic hazards. *Geol. Soc. Lond. Spec. Publ.* 441 (1), 71–120. <https://doi.org/10.1144/sp441.8>.
- Watkinson, I.M., Hall, R., Ferdian, F., 2011. Tectonic re-interpretation of the Banggai-Sula-Molucca Sea margin, Indonesia. *Geol. Soc. Lond. Spec. Publ.* 355 (1), 203–224. <https://doi.org/10.1144/sp355.10>.
- Wessel, P., Luís, J., Uieda, L., Scharroo, R., Wobbe, F., Smith, W.H.F., Tian, D., 2019. The Generic Mapping Tools Version 6. *Geochem. Geophys. Geosyst.* 20 (11), 5556–5564. <https://doi.org/10.1029/2019gc008515>.
- Wibowo, A., Supendi, P., Nugraha, A.D., 2020. Coulomb stress change of MW 7.5 Palu-Donggala Earthquake, Sulawesi (28 September 2018). *Jurnal Geofisika* 18 (1), 19. <https://doi.org/10.36435/jgf.v18i1.423>.
- Yeats, R., 2012. Southeast Asia, Australia, New Zealand, and Pacific Islands. In: *Active Faults of the World*. Cambridge University Press, Cambridge, pp. 448–500. <https://doi.org/10.1017/CBO9781139035644.011>.
- Zhang, X., Tien, C.Y., Chung, S.L., Maulana, A., Mawaleda, M., Chu, M.F., Lee, H.Y., 2020. A Late Miocene magmatic flare-up in West Sulawesi triggered by Banda slab rollback. *GSA Bull.* 132 (11–12), 2517–2528. <https://doi.org/10.1130/b35534.1>.
- Zhang, X., Huang, T.N., Chung, S.L., Maulana, A., Mawaleda, M., Tien, C.Y., Lee, H.Y., Liu, P.P., 2022. Late Eocene subduction initiation of the Indian Ocean in the North Sulawesi Arc, Indonesia, induced by abrupt Australian plate acceleration. *Lithos* 422–423, 106742. <https://doi.org/10.1016/j.lithos.2022.106742>.
- Zheng, T., Qiu, Q., Lin, J., Yang, X., 2023. Raised potential earthquake and tsunami hazards at the North Sulawesi subduction zone after a flurry of major seismicity. *Mar. Pet. Geol.* 148, 106024. <https://doi.org/10.1016/j.marpetgeo.2022.106024>.